

# UNCLASSIFIED

AD NUMBER
AD810823
NEW LIMITATION CHANGE
TO Approved for public release, distribution unlimited
FROM Distribution authorized to U.S. Gov't. agencies and their contractors; Critical Technology; Mar 1967. Other requests shall be referred to Air Force Rocket Propulsion Lab., Attn: RPPR-STINFO, Edwards AFB, CA 93523.
AUTHORITY
27 Oct 1971 per AFRPL ltr

THIS PAGE IS UNCLASSIFIED

63  
22  
63  
10  
00

# DOWNEY PLANT

ORDNANCE DIVISION

---

PROJECT SOPHY  
SOLID PROPELLANT HAZARDS PROGRAM

Technical Documentary Report No.  
AFRPL-TR-67-67

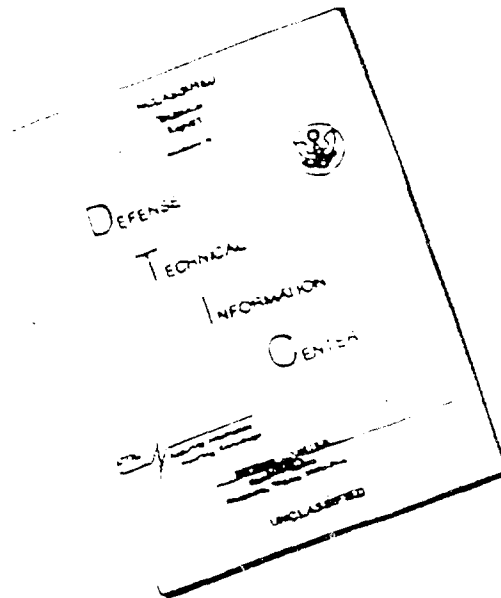
Progress Report On  
Contract AF 04(611)-10919

Report Number 0977-01(06)QP / March 1967 / Copy 70

---



# DISCLAIMER NOTICE



THIS DOCUMENT IS BEST  
QUALITY AVAILABLE. THE COPY  
FURNISHED TO DTIC CONTAINED  
A SIGNIFICANT NUMBER OF  
PAGES WHICH DO NOT  
REPRODUCE LEGIBLY.

AEROJET-GENERAL CORPORATION

Ordnance Division  
11711 Woodruff Avenue  
Downey, California

PROGRESS REPORT

PROJECT SOPHY  
SOLID PROPELLANT HAZARDS PROGRAM

Technical Documentary Report No.  
AFRPL-TR-67-67

Contract AF 04(611)-10919

0977-01(06)OP

Period Covered: 1 December 1966 - 28 February 1967

R. B. Elwell  
P. K. Salzman  
Prepared by: W. T. Weatherill

Date: 28 March 1967

Reviewed by: M. Nishibayashi  
M. Nishibayashi, Head  
Explosive Kinetics Dept.

No. of Pages: 61

Approved by: H. J. Fisher  
H. J. Fisher, Manager  
Research Division

Classification: UNCLASSIFIED

"This document is subject to special export controls and each transmittal to foreign governments or foreign nationals may be made only with prior approval of AFRPL (RPPR-STINFO), Edwards, California 93523."

## FOREWORD

This report was prepared by Aerojet-General Corporation, Downey, California, on Air Force Contract AF 04(611)-10919, which supports the USAF Solid Propellant Hazards Study Program (Project SOPHY), Project 63A00201. The period covered by this report is 1 December 1966 through 28 February 1967.

## ABSTRACT

Verification that the sustainment theory of critical geometry can be applied to an adulterated propellant different from that by which the theory was originally developed has been obtained from tests of square column and hollow-core cylindrical shapes. The effect of pulse width on the minimum shock pressure required to initiate detonation has been determined experimentally by flyer-plate tests. The initiation criteria for three different RDX-adulterated PBAN-type propellants have been determined. From these, the minimum shock pressure required to initiate detonation of unadulterated propellant is predicted to be approximately 20 kbar at critical diameter and 10 kbar at ideal diameter.

## CONTENTS

	<u>Page No.</u>
1. INTRODUCTION .....	1
2. SUMMARY .....	1
3. THEORY OF CRITICAL GEOMETRY .....	2
3.1 Technical Discussion -- Phase 1 Subtasks .....	2
3.2 Technical Discussion -- Phase 2 Subtasks .....	2
4. PROPELLANT DEFECTS STUDY .....	44
5. FUTURE WORK .....	44
5.1 Plexiglas Hugoniot .....	44
5.2 Evaluation of Initiation Criterion .....	45
REFERENCES .....	46
DISTRIBUTION .....	47

## ILLUSTRATIONS

<u>Figure No.</u>		<u>Page No.</u>
1.	Equation of State of Aluminum and PBAN Propellant . . . . .	7
2.	Pressure in PBAN Propellant as a Function of Flyer Plate Velocity . . . . .	8
3.	Pulse Width of Shock Wave in PBAN Propellant . . . . .	9
4.	Experimental Test Configuration . . . . .	11
5.	Test Setup Using Flash X-Ray . . . . .	12
6.	Flyer Plate Velocity vs Wt/Sq In. of Detasheet-C (Aluminum Flyer Plate 0.0625 in. by 5 in. by 5 in.) . . . . .	13
7.	Flyer Plate Velocity vs Wt/Sq In. of Detasheet-C (Aluminum Flyer Plate 1/8 in. by 5 in. by 5 in.) . . . . .	14
8.	Flyer Plate Velocity vs Wt/Sq In. of Detasheet-C (Flyer Plate 3/16 in. by 5 in. by 5 in.) . . . . .	15
9.	Flyer Plate Velocity vs Wt/Sq In. of Detasheet-C (Aluminum Flyer Plate 0.250 in. by 5 in. by 5 in.) . . . . .	16
10.	Flyer Plate Velocity vs Thickness of Flyer Plate (Test Materials: Aluminum Flyer Plate, Layers of Detasheet C-1, and Steel Platform) . . . . .	17
11.	Angle of Tilt Required to Obtain Simultaneity of Impact at Target as a Function of the Aluminum Flyer Plate Velocity . . . . .	18
12.	Effect of Pulse Width on Shock Pressure Required to Initiate Detonation of 4-in. Diameter Samples of AAB-3189 . . . . .	21
13.	Effect of Pressure-Pulse Duration on the Initiation to Detonation of PBAN Propellant (9.2 Wt % RDX) 4 in. OD by 4 in. Long . . . . .	22



## ILLUSTRATIONS (Continued)

<u>Figure No.</u>		<u>Page No.</u>
14.	Attenuation in 8-in. Squares of Stacked Plexiglas Plates . . . . .	27
15.	Attenuation in 10-in. Squares of Stacked Plexiglas Plates . . . . .	28
16.	Attenuation in 12-in. Squares of Stacked Plexiglas Plates . . . . .	29
17.	Attenuation in 20-in. Squares of Stacked Plexiglas Plates . . . . .	30
18.	Attenuation in 24-in. Squares of Stacked Plexiglas Plates . . . . .	31
19.	Attenuation in 42-in. Squares of Stacked Plexiglas Plates . . . . .	32
20.	Correlation of Shock Pressure Attenuation Data . . . . .	33
21.	Initiation Criterion for AAB-3189 . . . . .	38
22.	Initiation Criterion for AAB-3225 . . . . .	39
23.	Initiation Criterion for AAB-3267 . . . . .	40
24.	Normalized Initiation Criterion . . . . .	41

## 1. INTRODUCTION

This quarterly report is the sixth of a series of reports partially fulfilling Contract AF 04(611)-10919, Large Solid-Propellant Boosters Explosives Hazard Study Program. The purpose of this program is to gain additional knowledge and to develop new techniques for analyzing the explosives hazard and damage potential of large solid-propellant rocket motors.

The objectives of this program are (1) to determine the influence of grain shape on propellant detonability and sensitivity, (2) to determine the critical diameter of a typical solid-composite rocket-motor propellant, (3) to determine what changes a solid-propellant grain might undergo when exposed to operational mishaps, and (4) to develop methods to simulate and characterize these changes.

## 2. SUMMARY

The critical-geometry sustainment theory has been applied to square columns and circular- and cross-core cylinders of AAB-3225. The experimental results from tests at the statistical 3-sigma limits around the predicted mean critical geometries have agreed with theory. Testing in this subtask will be completed by mid-May.

The effect of pulse width on the shock pressure required to initiate detonation has been investigated experimentally using 4-in. diameter AAB-3189 propellant samples and aluminum flyer plates. The data suggest that (1) minimum shock pressure required to initiate detonation decreases as the pulse width is increased, but (2) there is a lower limit to the minimum initiating pressure, below which initiation of detonation cannot occur with any pulse width.

Card-gap sensitivity test results, obtained at sample diameters from near-critical to near-ideal, indicate that with less RDX in the formulation, a lower shock pressure will initiate detonation of a near-critical sample. However, at the ideal-diameter region, the sensitivities of these propellants are essentially indistinguishable from one another. This set of observations suggests that the sensitivity of unadulterated propellant is rather high; i. e., full-diameter shock pressures in the neighborhood of 10 to 15 kbars may produce detonation.

New areas of investigation are discussed, which have been added to the technical objectives of this contract, to be performed within a 2-1/2 month extension granted by the Air Force contracting officer.

### 3. THEORY OF CRITICAL GEOMETRY

#### 3.1 TECHNICAL DISCUSSION -- PHASE 1 SUBTASKS

##### 3.1.1 Detonation Velocity as a Function of Size (Subtask 3.2.3\*)

This subtask is concerned with determining whether the nonideal detonation behavior of solid composite propellant can be described by the modified Jones expression that was used in the development of the Aerojet detonation model (Reference 2). Data have been acquired on the detonation velocities of several sizes of cylinders cast from AAB-3189 propellant (adulterated with 9.2% RDX) and AAB-3225 (7.1% RDX). The complete analysis of these data is almost finished. The results will be reported in the next monthly report, to be distributed in April.

#### 3.2 TECHNICAL DISCUSSION -- PHASE 2 SUBTASKS

##### 3.2.1 Verification of Theory (Subtask 3.3.3)

This subtask is concerned with determining whether the sustainment theory of critical geometry can be applied to a propellant that is different from the formulation used during its initial evaluation. The original critical geometry concept stated that for a given material there is one value of the critical geometry that defines the critical size of any shape sample, below which detonation cannot be achieved. This value is equal to the critical diameter. For any shape it is equal to four times the area divided by the total perimeter of the cross-section that is normal to the direction of the reaction wave. This hypothesis was evaluated by experimental investigations during SOPHY I and SOPHY II, under Contracts AF 04(611)-9945 and AF 04(611)-10919, respectively, using AAB-3189 propellant, which is an adulterated PBAN-type propellant containing

---

\*Subtask number refers to the paragraph number in the Program Plan (Reference 1) that locates the description of that particular series of tests.

9.2% RDX by weight. From the results of these tests it was concluded that the theory predicted larger sizes to be critical than were actually found. Redefining critical geometry as the ratio of four times the area and the perimeter, for each shape, it was stated that for nonperforated (i. e., solid cross-section) shapes, the critical geometry is 92 to 95% of the critical diameter and for perforated shapes it is 88% of the critical diameter (Reference 3).

Under Subtask 3.2.2, the standard deviation in the critical diameter test results for samples cast from AAB-3225 (7.1% RDX) was found to be 0.1 in. (Reference 4). This study was made so that it would be possible to design the series of tests required in the critical geometry verification, which used the AAB-3225 material. Mean critical geometries were calculated for AAB-3225 in square columns, circular-core cylinders, and cross-core cylinders. Samples were cast at sizes that were three standard deviations below the predicted mean critical size and three standard deviations above. This approach was adopted instead of actually determining the mean critical geometries because it required many less samples and, consequently, was less costly.

The circular-core cylinders were tested in two series: one with a 3-in. diameter core and the other with a 6-in. diameter core. The cross-core samples similarly were divided into two series, with core sizes comparable to the circular-core sizes.

All samples are instrumented with ionization-type probes to obtain data from which the velocity of the reaction wave is computed. The criterion for sustainment with the square shape is the stabilization of the detonation velocity over the lower half of the charge, which originally is four times as long as the side of the square cross-section. Hollow-core cylinders have presented a special problem in critical geometry tests because of the formation of central cavity jetting and the influence of the jet on the detonative behavior of the grain (Reference 3). The concept of pseudocritical geometry was introduced to allow full evaluation of the critical-geometry theory by essentially compensating for the abnormal behavior that is characteristic of the hollow cylinder. If sustainment is clearly evident over the upper portion of the charge, it is assumed that the charge is above the pseudocritical geometry. This principle must be applied only when the test conditions are so established as to ensure that (1) the sample is not highly overboosted, and (2) the jet is prevented from being formed by the booster. The first condition simplifies analysis of the data because a size that is below the pseudocritical

size will very quickly show attenuation of the shockwave, and a larger size (above pseudocritical) will propagate at a sustained velocity more quickly. The second condition delays the formation of the jet and thereby prolongs the period where jet-interference is absent.

For the test design adopted in this subtask, the larger sizes of any series are expected to detonate, and the smaller sizes to fail. The results show complete agreement with the predictions (Table 1). With the hollow-core samples, the ones that did satisfy the requirements for being above the pseudocritical size showed sustained propagation for most of the sample length. In the 8-in. OD samples, the sustainment lasted for 20 to 36 in.; in the 11-in. OD samples, for 35 to 40 in.

In cases where the hollow cylinders did not satisfy the requirements (i. e., the no go's) the velocity of the reaction wave at the middle of the web attenuated to below critical velocity within 2 in.

As shown in Table 1, all tests have not yet been performed. The larger size samples originally had been scheduled for testing at the Aerojet ordnance laboratory in Chino with all the others, but the large number and range of the burning propellant fragments have forced cancellation of this schedule and substitution of the 1-36D area at AFRPL, Edwards, as the test site. The tests will be completed within a few weeks.

### 3.2.2 Initiation Pressure vs Pulse Width (Subtask 3.3.4)

The objective of this subtask is to investigate the relationship between the shock pressure required to initiate detonation and the pulse-width of the shock wave. This study is a preliminary study for the broadened initiation criterion that considers shock pressure, shockwave area, and pulse width to be the three determining parameters of initiation to detonation. In the study of the pressure-pulse width relationship, the flyer-plate technique was applied.

#### 3.2.2.1 Background

When one condensed material impacts another, the shock pressure and pulse duration are calculated from knowledge of the test conditions and the Hugoniot equations of state of the two materials. In this particular

Table 1. Critical Geometry -- Verification of  
Sustainment Theory, Using AAB-3225.

Shape	Inner Dimension (in.)	Outer Dimension (in.)	Test Result	Detonation Velocity	Test No.
Square column	N/A	4-1/2 x 4-1/2	No-go	N/A	3.3.3.3
		4-1/2 x 4-1/2	No-go	N/A	3.3.3.14
		4-1/2 x 4-1/2	No-go	N/A	3.3.3.15
		4-1/2 x 4-1/2	No-go	N/A	3.3.3.17
		5-1/8 x 5-1/8	Go	4.11	3.3.3.5
		5-1/8 x 5-1/8	Go	4.19	3.3.3.9
		5-1/8 x 5-1/8	Go	4.11	3.3.3.16
Circular-core cylinder	3	7-1/4	No-go	N/A	3.3.3.1
		7-1/4	No-go	N/A	3.3.3.6
		7-1/4	No-go	N/A	3.3.3.22
		7-1/4	No-go	N/A	3.3.3.23
		8	Go	4.29	3.3.3.2
		8	Go	4.35	3.3.3.11
		8	Go	4.21	3.3.3.24
		8	Go	4.29	3.3.3.25
	6	10-1/4	No-go	N/A	3.3.3.13
		11	Go	4.43	3.3.3.19
Cross-core cylinder	3 x 3 cross	7-1/4	No-go	N/A	3.3.3.8
		7-1/4	No-go	N/A	3.3.3.10
		7-1/4	No-go	N/A	3.3.3.20
		7-1/4	No-go	N/A	3.3.3.21
		8	Go	4.39	3.3.3.5
		8	Go	4.34	3.3.3.12
		8	Go	4.40	3.3.3.26
		8	Go	4.49	3.3.3.27
	6 x 6 cross	11	Go	4.40	3.3.3.18

case, aluminum plates were propelled at 4-in. diameter samples of AAB-3189. Knowing the flyer-plate velocity, the shock pressure generated on impact at the plate-propellant interface can be determined by the Hugoniot reflection method (Reference 5). The shock velocity in the aluminum,  $U_{Al}$ , and in the propellant,  $U_{PBAN}$ , can then be calculated directly from the Hugoniots of these materials.

The time of contact, neglecting any attenuation of the shock wave in the flyer plate, is given by

$$t = \frac{2x}{U_{Al}} \quad (1)$$

where  $t$  = contact time and  $x$  = flyer-plate thickness. The duration time of the pulse entering the propellant will be equal to  $t$ , and if attenuation in the propellant is neglected,

$$t = \frac{w}{U_{PBAN}} \quad (2)$$

where  $w$  = the pulse width in the propellant. By equating Equations 1 and 2 and rearranging,

$$w = \frac{2xU_{PBAN}}{U_{Al}} \quad (3)$$

The Hugoniot reflection method is shown in Figure 1 for various values of  $\mu_f$ , the particle velocity of the flyer plate. Shock pressures transmitted at impact as a function of  $\mu_f$  are shown in Figure 2, and the pulse width (mm) as a function of  $\mu_f$  and  $x$  is shown in Figure 3.

### 3.2.2.2 Test Description

Aluminum flyer plates 5-in. square were propelled at 4-in. diameter cylindrical samples of AAB-3189 (critical diameter = 2.7 in.). The pulse width and shock pressure were varied from test to test by proper selection of flyer plate velocity and thickness.

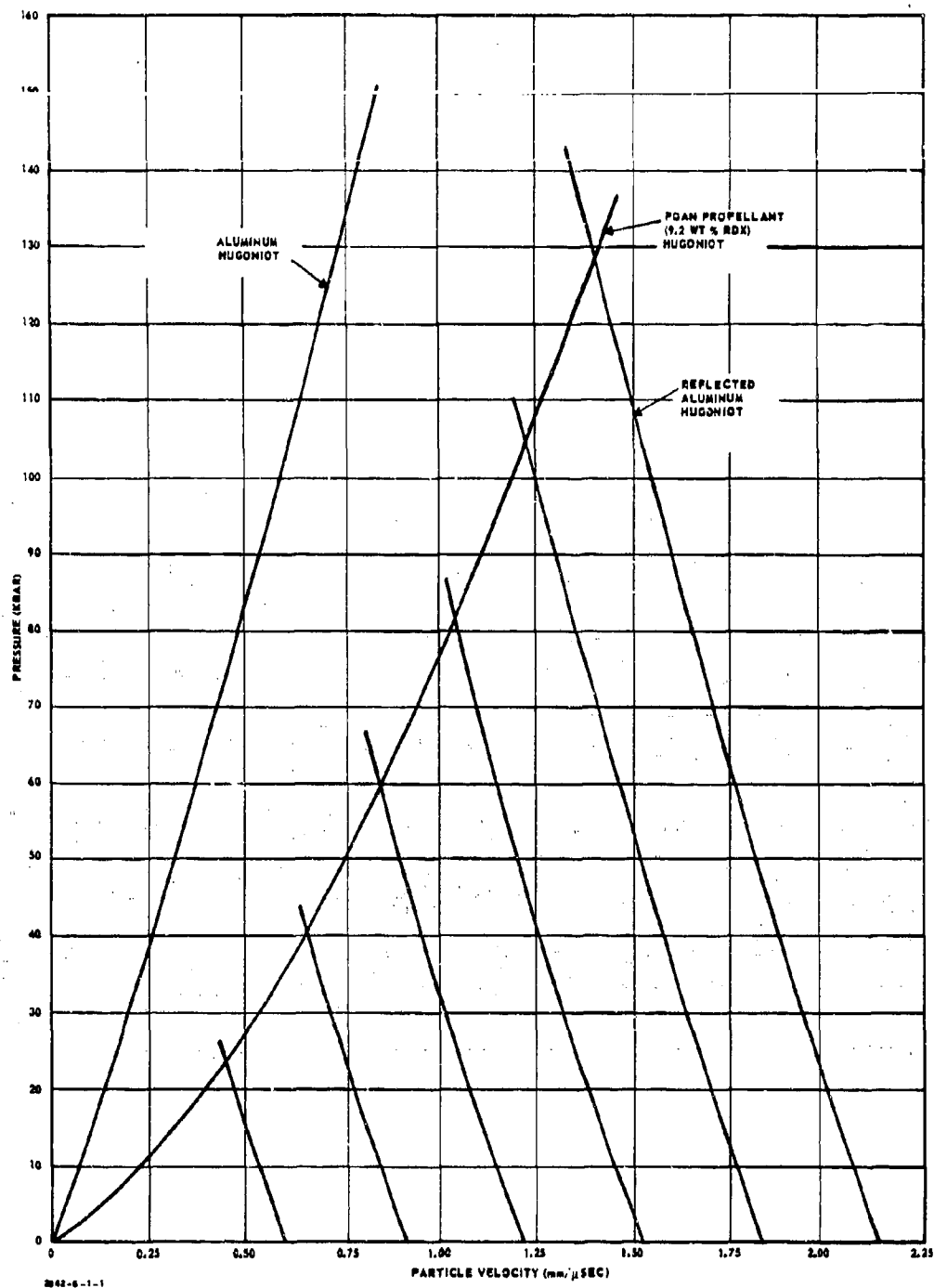


Figure 1. Equation of State of Aluminum and PBAN Propellant.



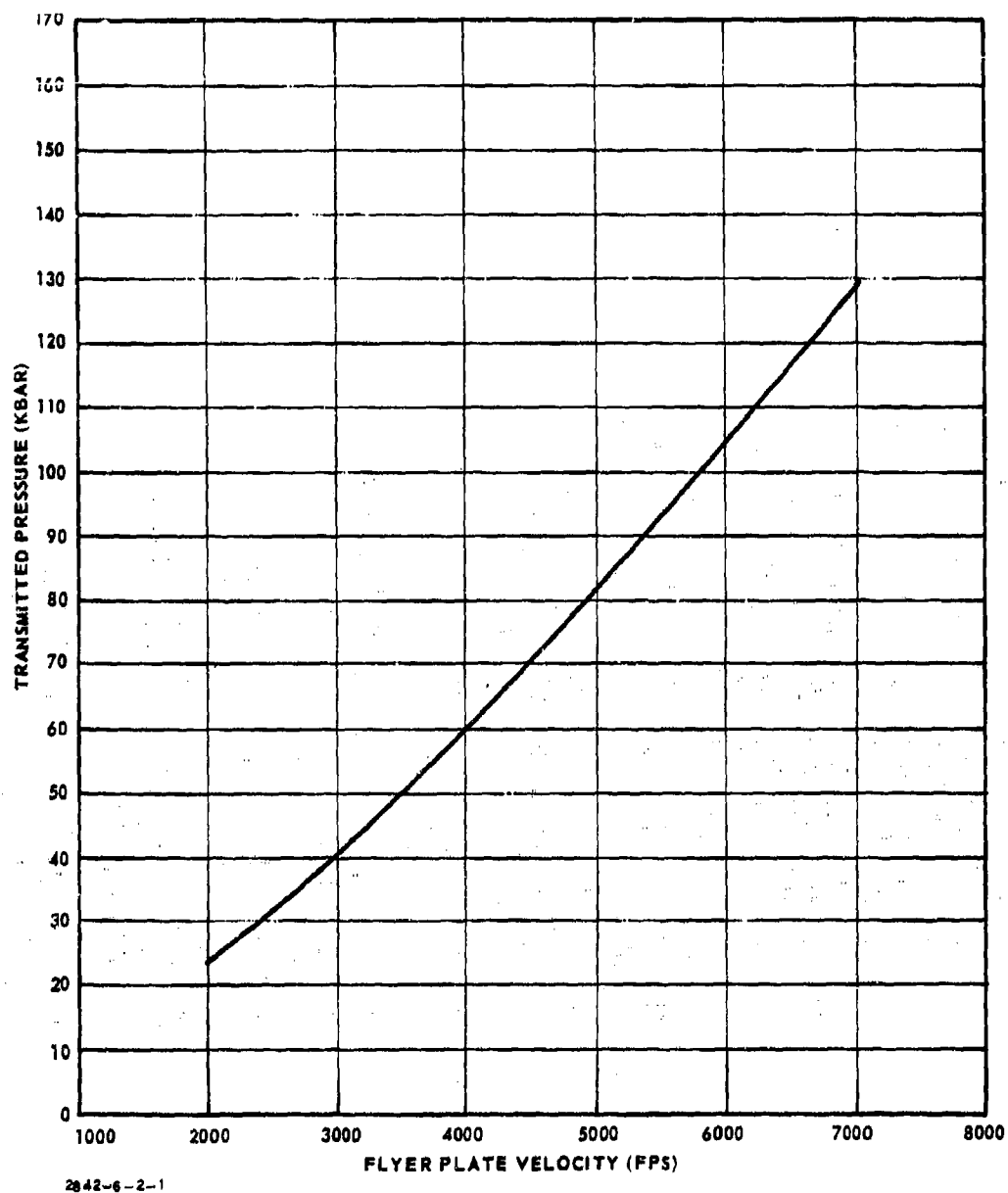
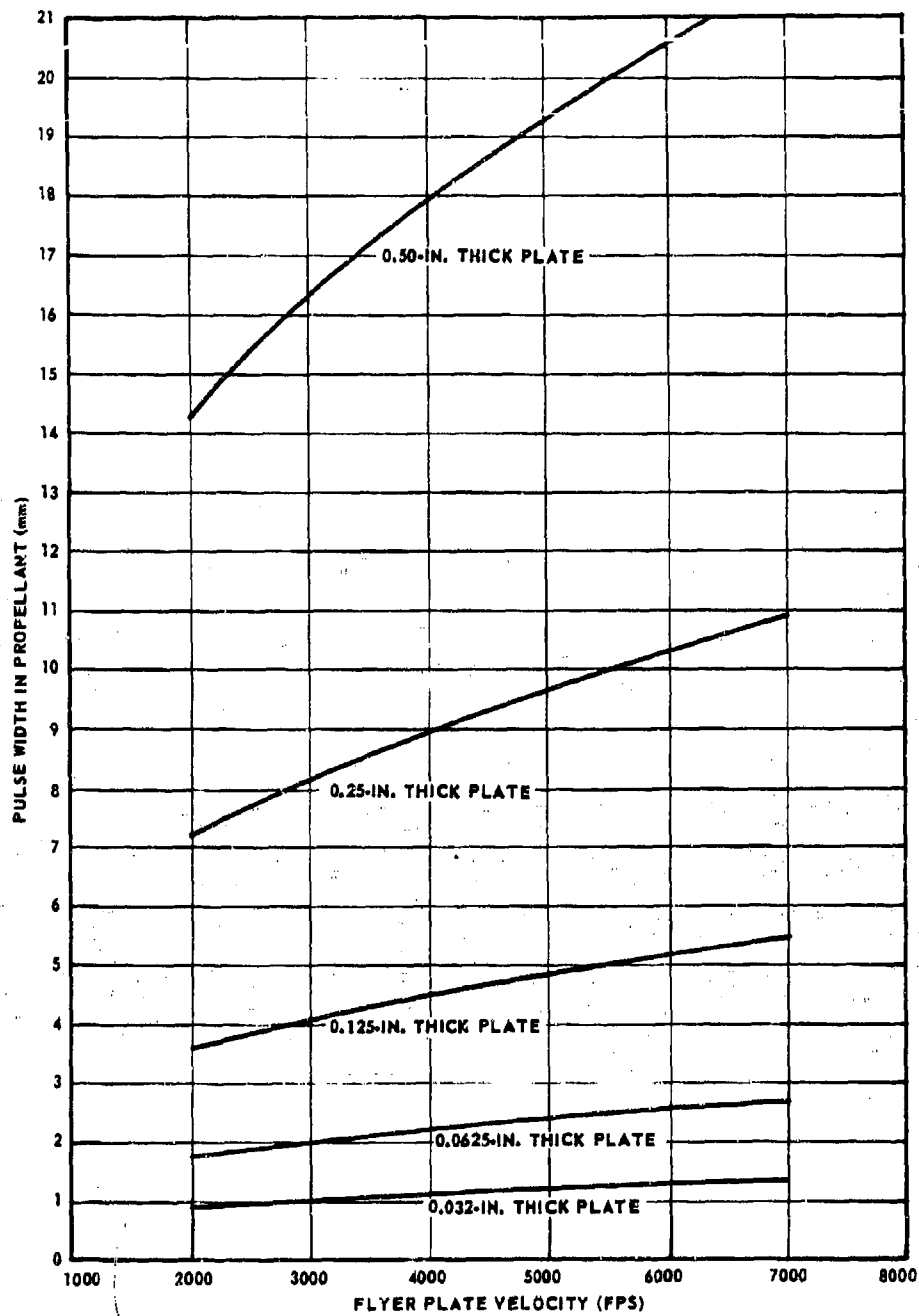


Figure 2. Pressure in PBAN Propellant As a Function of Flyer Plate Velocity.



2042-6-3-1

Figure 3. Pulse Width of Shock Wave in PBAN Propellant.

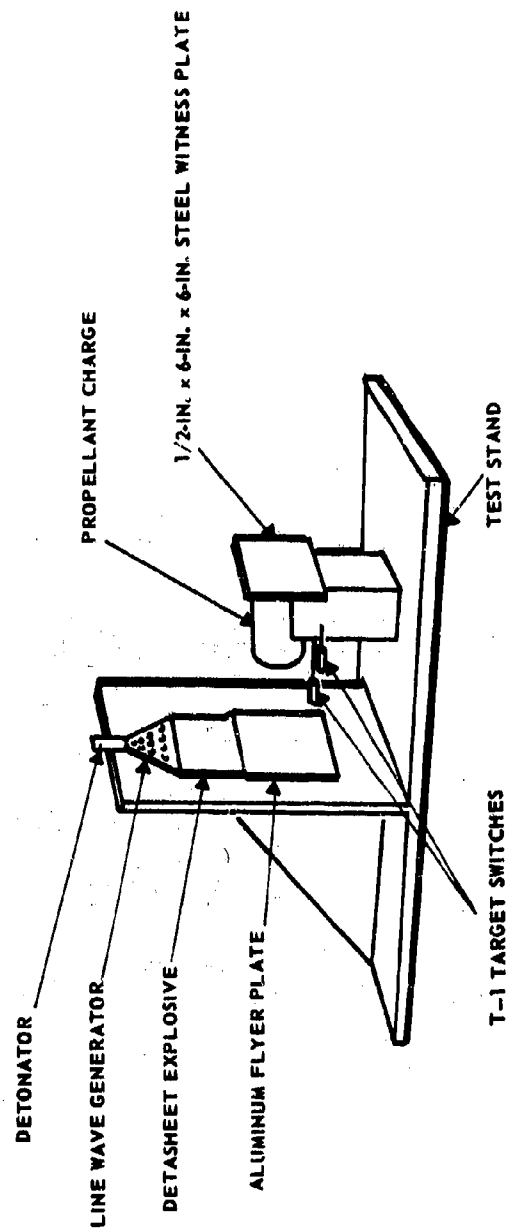
Figure 4 shows the test orientation. The T-1 target switches are located in the path of the plate, at a measured separation from each other, so that the velocity of the plate can be determined. A 6- by 6- by 1/2-in. steel plate placed against the rear of the acceptor charge functions as a witness plate to facilitate interpretation of the test results.

### 3.2.2.3 Flyer-Plate Technique

An experimental method was developed to accelerate aluminum flyer plates to velocities ranging from 2000 to 7000 fps. This velocity range is required to obtain a shock pressure range suitable for the propellant initiation-to-detonation study. A flash X-ray system is used to monitor the flight of the flyer plate. The flyer-plate velocity and the angle of tilt required to obtain simultaneous impact of the flyer plate against a target were then determined from the radiographs. The experimental setup is shown in Figure 5.

Initially, the tests were performed with a single sheet of Detasheet C explosive. Only a limited amount of Detasheet of different thicknesses was available at the Chino Hills Ordnance Laboratory, and a 10 to 12-week lead time is required to obtain the explosive from the vendor. Therefore, multiple layers of Detasheet C-1 (0.042-in. thick) explosive were used. The flyer-plate velocities obtained with the multiple layers of explosive were different from the velocities obtained with one layer of the thicker Detasheet. The flyer-plate velocities, obtained as a function of the explosive weight per square inch, are shown graphically in Figures 6 through 9. A family of curves describing flyer-plate velocity as a function of plate thickness, using 1 to 4 layers of Detasheet C-1, is shown in Figure 10. The angle of tilt of the flyer plate was determined to be a function of plate velocity. The data are shown in Figure 11.

During the program, it was found that the flyer-plate velocity, using a specific explosive weight per square inch, could be reduced by using a plywood test stand instead of steel. This increased the range of flyer-plate velocities obtainable with the limited supply of explosives.



28 42-6-4-1

Figure 4. Experimental Test Configuration.

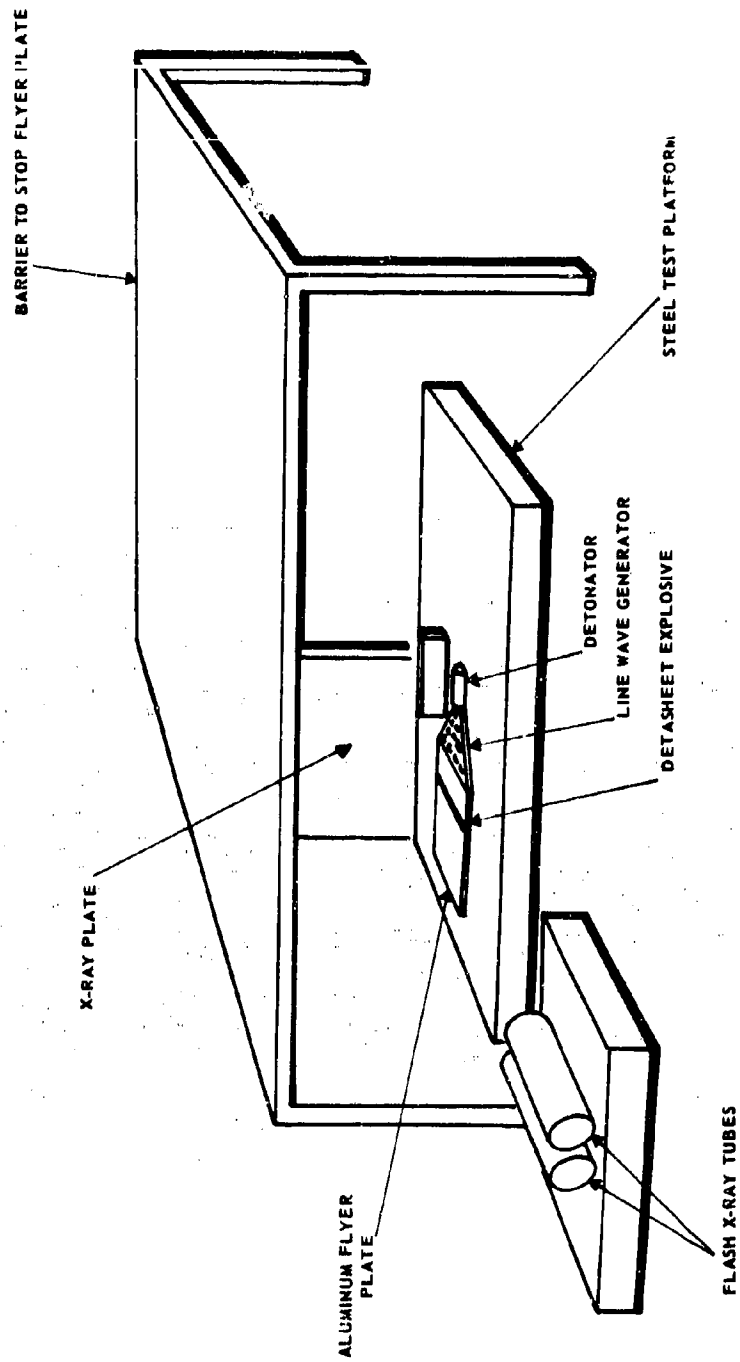


Figure 5. Test Setup Using Flash X-Ray.

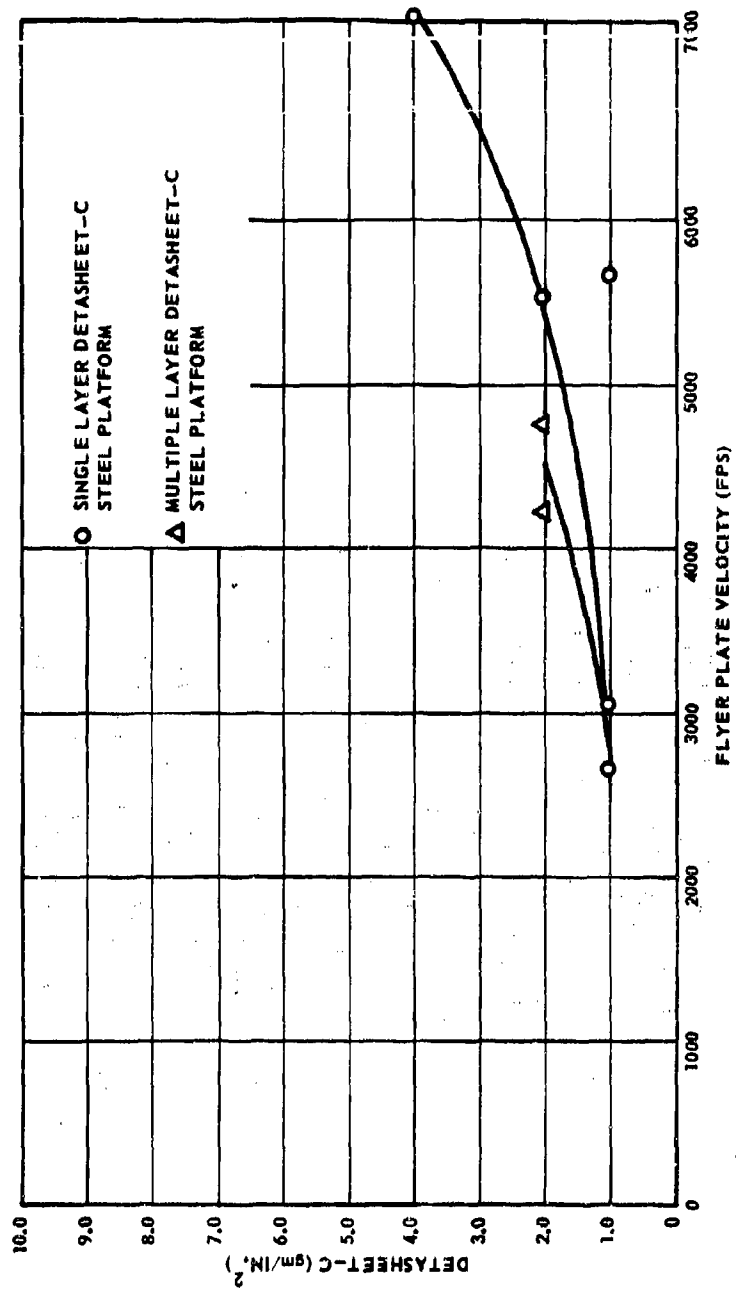


Figure 6. Flyer Plate Velocity vs Wt/Sq In. of Detasheet-C.  
(Aluminum Flyer Plate 0.0625 in. by 5 in. by 5 in.)

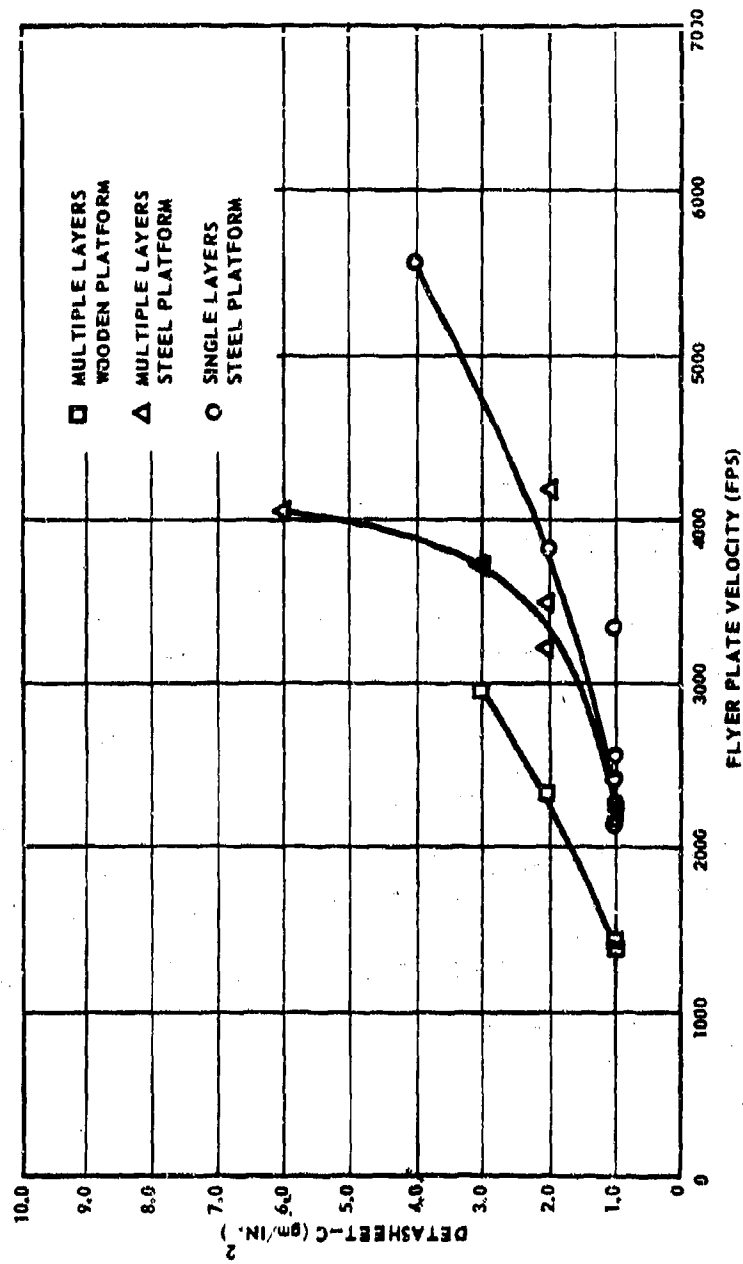


Figure 7. Flyer Plate Velocity vs Wt/Sq In. of Detasheet-C.  
(Aluminum Flyer Plate 1/8 in. by 5 in. by 5 in.).

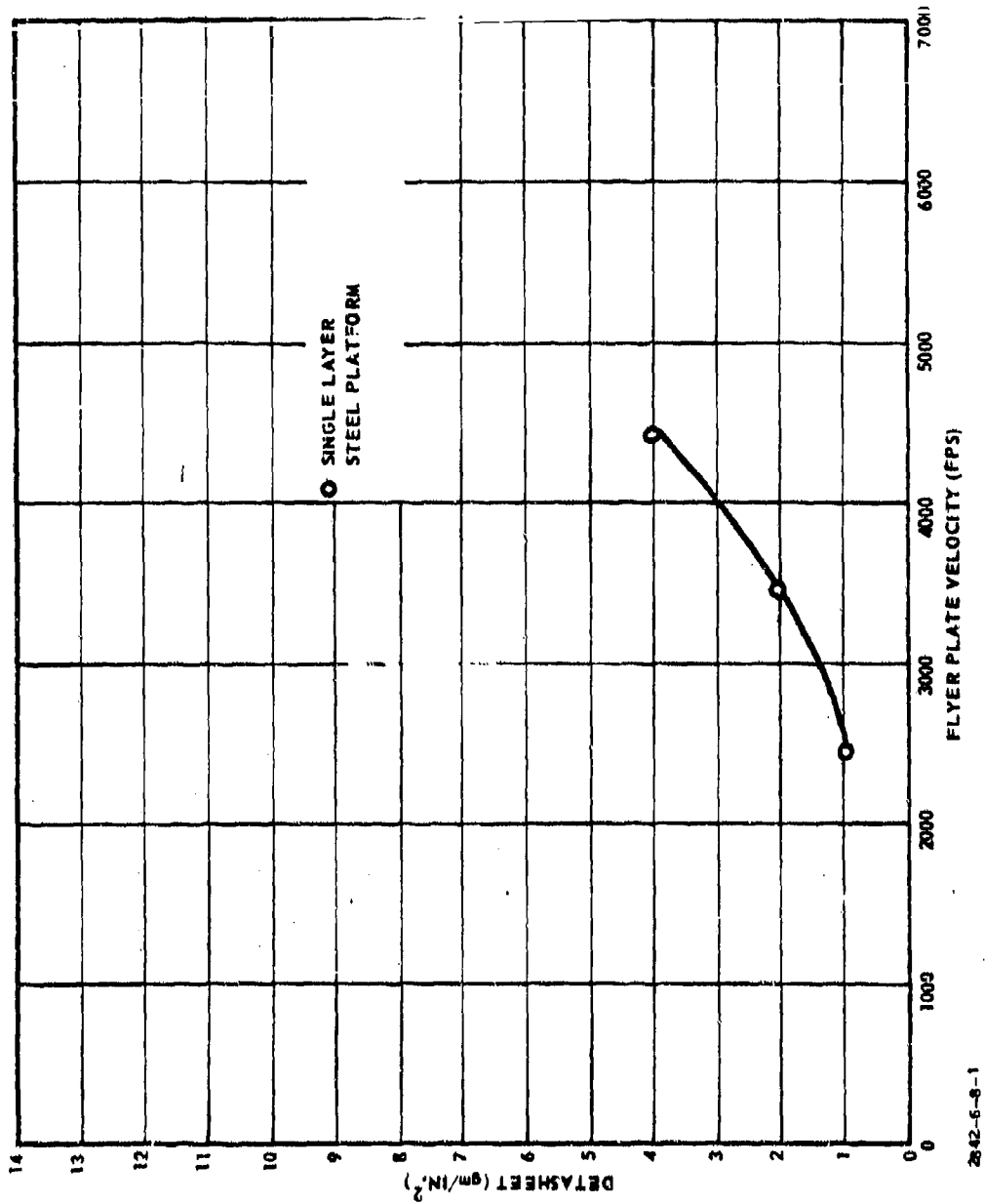


Figure 8. Flyer Plate Velocity vs Wt/Sq In. of Detasheet-C.  
(Flyer Plate 3/16 in. by 5 in. by 5 in.).



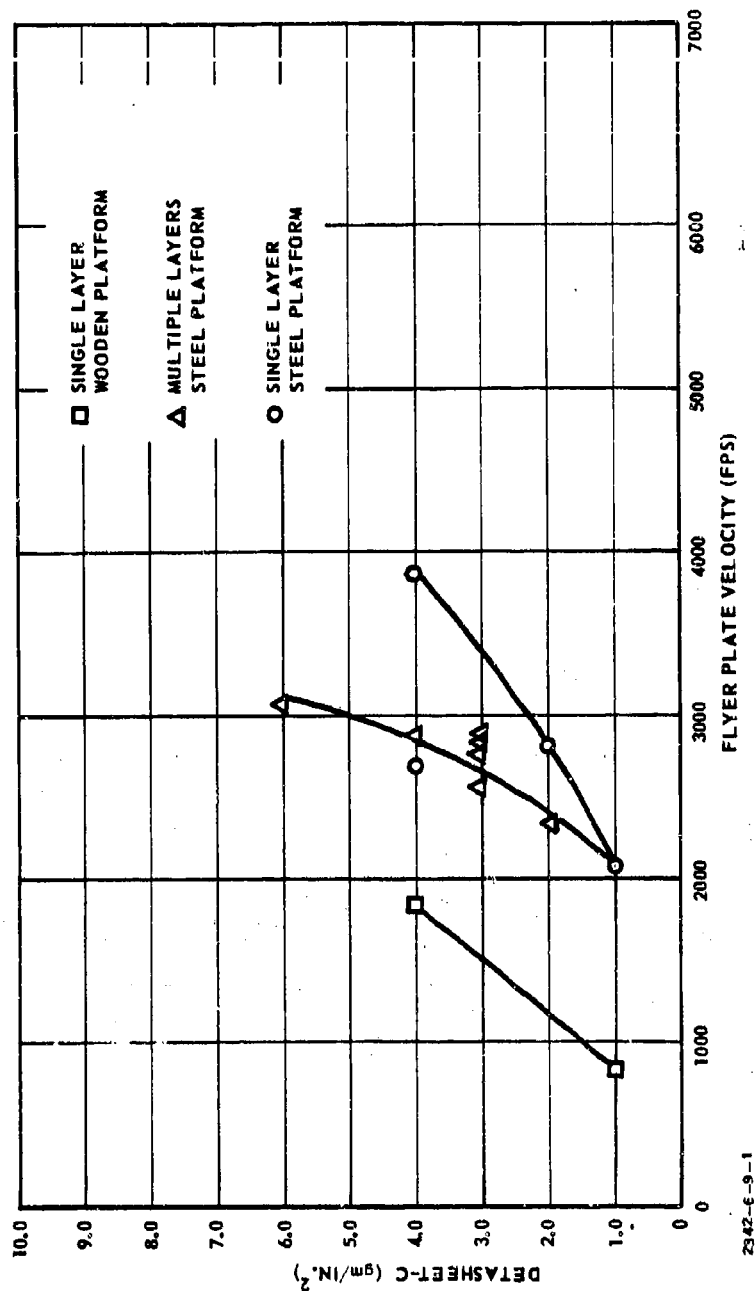


Figure 9. Flyer Plate Velocity vs Wt/Sq In. of Detasheet-C.  
(Aluminum Flyer Plate 0.250 in. by 5 in. by 5 in.)

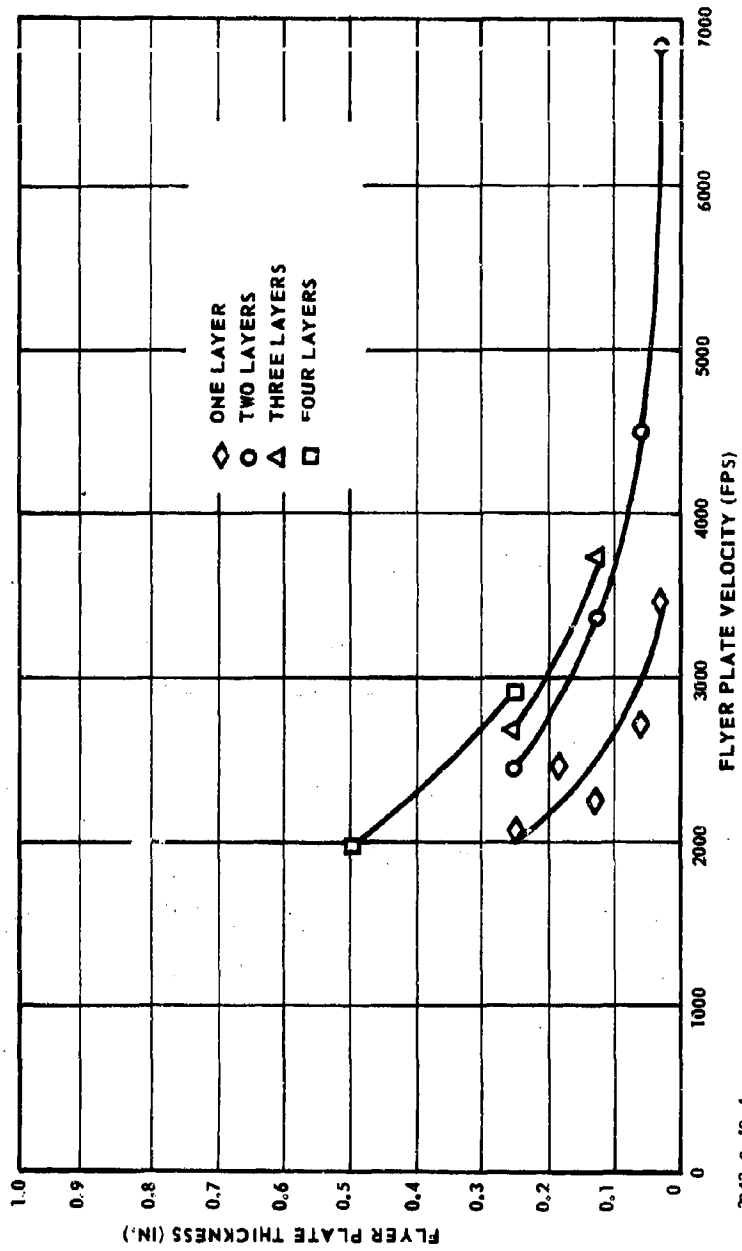


Figure 10. Flyer Plate Velocity vs Thickness of Flyer Plate.  
(Test Materials: Aluminum Flyer Plate, Layers of Detasheet C-1,  
and Steel Platform).

2842-6-10-1

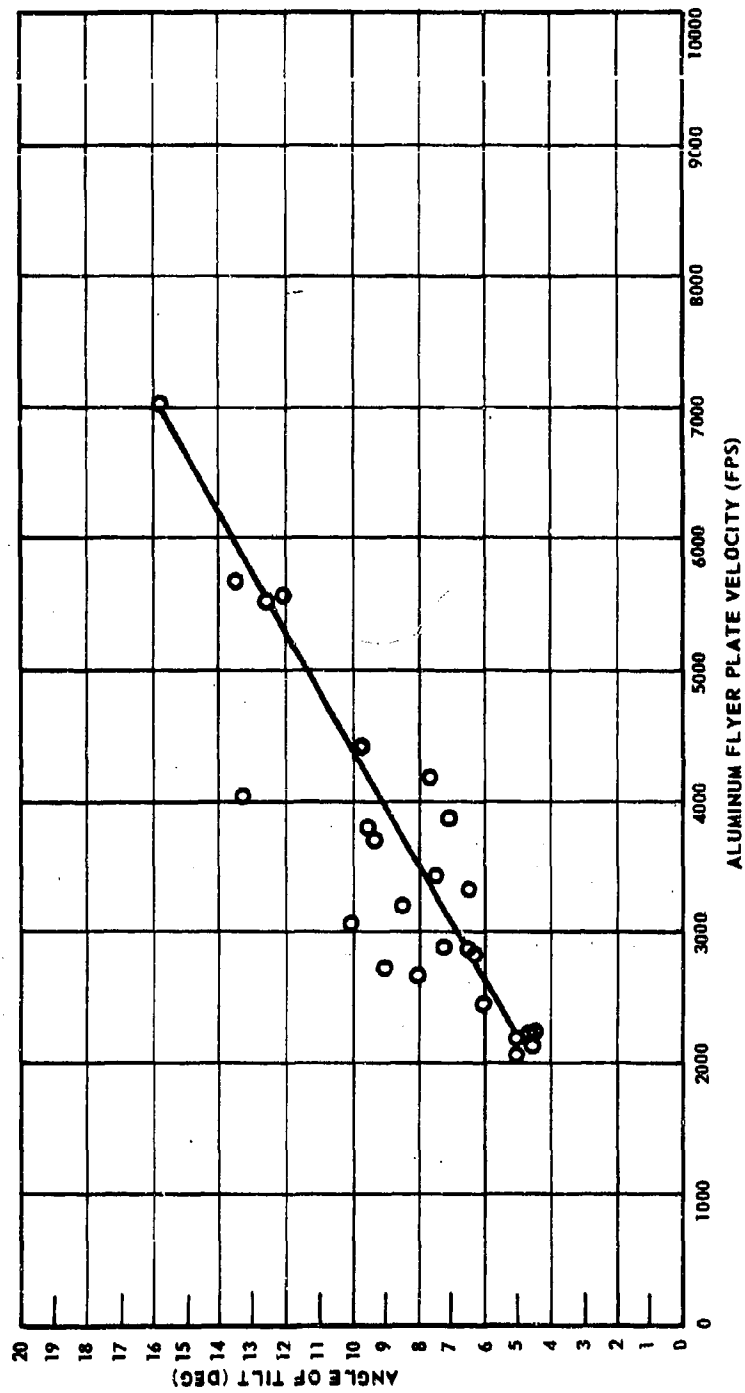


Figure 11. Angle of Tilt Required to Obtain Simultaneity of Impact at Target as a Function of the Aluminum Flyer Plate Velocity.

28 42-6-11-1

#### 3.2.2.4 Results

Sixteen tests were conducted after the developmental experiments were concluded. Aluminum plates from 1/32 to 1/2-in. thick were flung at velocities from 1868 to 6897 fps. The results of these tests are given in Table 2 and Figures 12 and 13. Examination of the figures reveals an expected relationship between the shock pressure and pulse width required to initiate detonation. Pulses of smaller width require higher pressure to achieve initiation of the acceptor. It is furthermore indicated that a minimum pressure exists, below which initiation is impossible with any width pulse. For the 4-in. diameter samples, this minimum pressure is near 30 kbar.

#### 3.2.3 Initiation Pressure vs Diameter (Subtask 3.3.5)

The purpose of this subtask is to determine the initiation criteria for adulterated propellants, with the objective of extrapolating these to postulate an initiation criterion for unadulterated propellant. The initiation criterion in its simplest form is defined as the region in the pressure-diameter plane that includes all points with coordinates greater than  $[P^+(d), d]$ . Here,  $P^+$  (P-cross) is the minimum shock pressure required to initiate detonation of a cylindrical sample of diameter  $d$ .  $P^+$  is a function of  $d$ , indicated by  $P^+(d)$ , and this function is defined by determining  $P^+$ 's at various  $d$ 's.

The initiation criterion can be expressed similarly with the shock wave area  $A$  substituted for  $d$ . This permits the concept to be applied to non-cylindrical shapes. As indicated in Section 3.2.2, the initiation criterion should also include pulse width as a variable, to be realistically meaningful. Therefore, the results of the tests described in this section do not constitute full definition of the initiation criterion. In the absence of evidence to the contrary, it has been assumed that the pulse width of the shock wave entering the samples from the Plexiglas attenuator does not change sufficiently with length of Plexiglas to jeopardize the assumption that the initiation criteria shown here are in the  $P, d$  plane and not a projection onto that plane.

Table 2. Results of Flyer-Plate Tests.

Test Number	Detasheet Explosive	Flyer Plate Thickness (in.)	Distance Between Pins (in.)	Time Between Pulses (μsec)	Velocity (fps)	Pressure (kbar)	Pulse Width in Propellant (mm)	Time (μsec)	Detonation of Propellant	Test Stand
3.3.4.46	Two-thickness C-1	1/8	0.87	20.7	3502	49.5	4.25	1.25	Yes	Steel
3.3.4.47	One-thickness C-1	1/8	1.07	34.6	2577	32.5	3.85	1.21	No	Steel
3.3.4.48	Three-thickness C-1	1/4	1.21	35.3	2857	37.5	7.95	2.44	Yes	Steel
3.3.4.49	Two-thickness C-1	1/4	1.12	39.7	2351	28.8	7.45	2.36	No	Steel
3.3.4.50	Two-thickness C-1	1/8	0.82	29.6	2309	28.2	3.71	1.18	No	Plywood
3.3.4.51	One-thickness C-1	1/16	0.93	27.2	3002	40.5	2.02	0.61	No	Steel
3.3.4.52	Three-thickness C-1	1/8	1.01	28.7	2933	39.5	4.45	1.35	No	Plywood
3.3.4.53	Two-thickness C-1	1/16	1.02	17.6	4775	76	2.38	0.64	Yes	Steel
3.3.4.54	One-thickness C-4	1/4	1.04	46.4	1865	21.5	7.00	2.31	No	Plywood
3.3.4.55	Three-thickness C-1	1/4	0.79	25.4	2592	53	7.70	2.40	Yes	Steel
3.3.4.56	Two-thickness C-1	1/16	1.01	20.0	4208	64	2.27	0.64	Yes	Steel
3.3.4.57	Four-thickness C-1	1/2	1.29	54.3	1980	23.5	14.2	4.62	No	Steel
3.3.4.58	One-thickness C-1	0.032	0.98	23.3	3505	49.5	2.12	0.62	No	Steel
3.3.4.59	Two-thickness C-1	0.032	1.44	17.4	6857	126	1.40	0.34	Yes	Steel
3.3.4.60	Five-thickness C-1	1/2	1.22	46.2	2201	26.5	14.7	4.73	No	Steel
3.3.4.61	Six-thickness C-1	1/2	1.29	33.6	3199	43.5	16.55	4.97	Yes	Steel

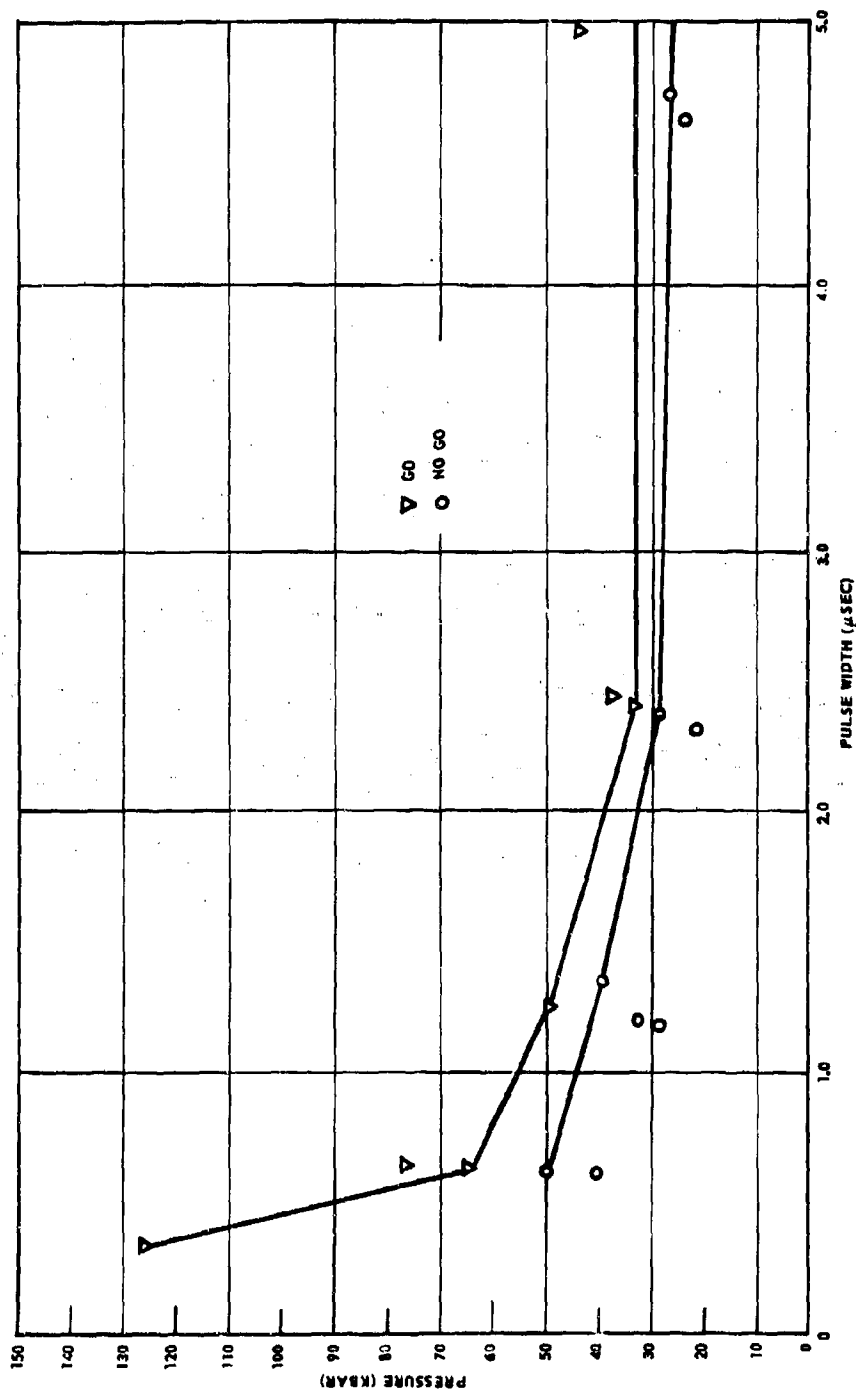
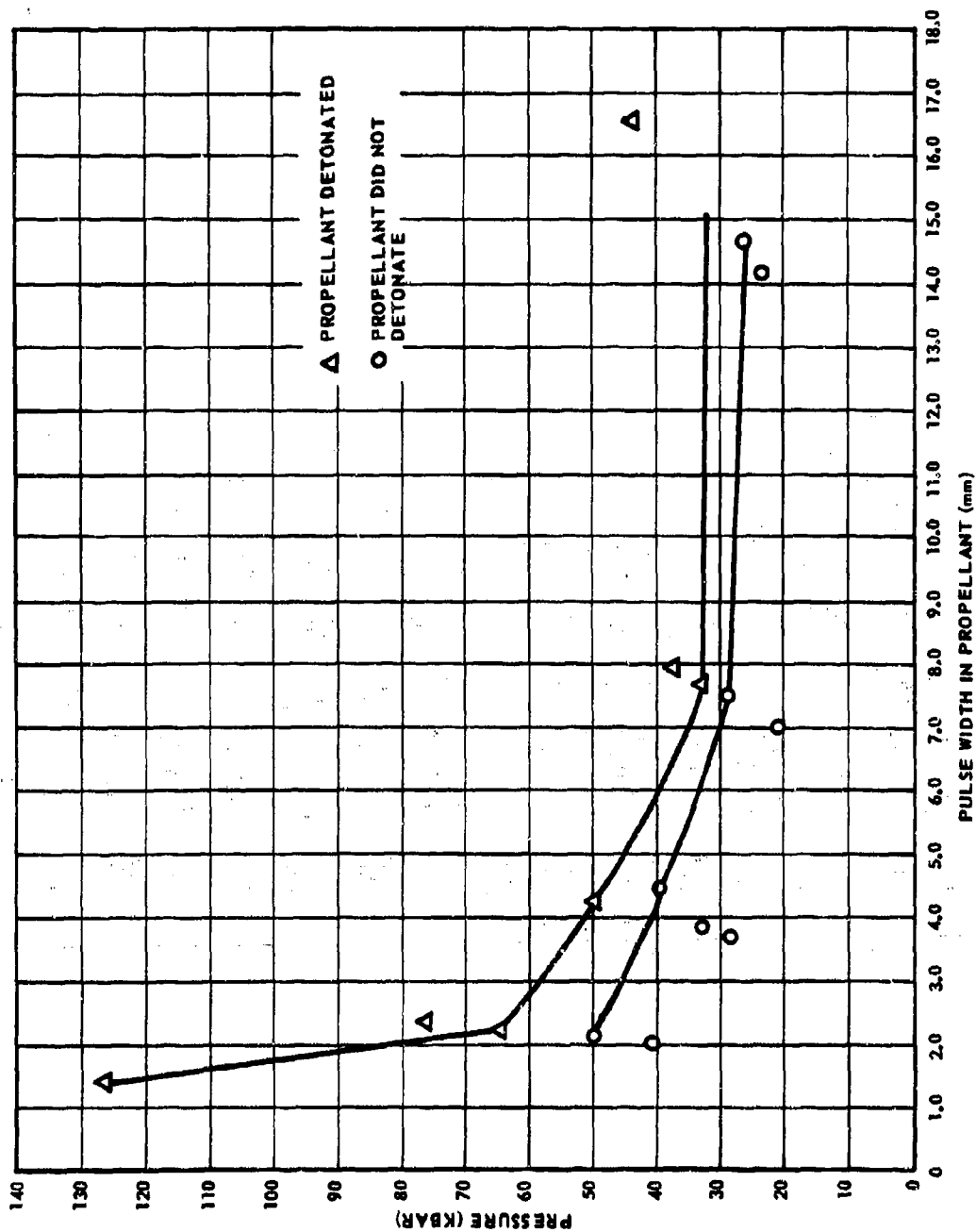


Figure 12. Effect of Pulse Width on Shock Pressure Required to Initiate Detonation of 4-in. Diameter Samples of AAB-3189.



2842-6-13-1

Figure 13. Effect of Pressure-Pulse Duration on the Initiation to Detonation of PBAN Propellant (9.2 Wt % RDX) 4 in. OD by 4 in. Long).

The estimation of the initiation criterion requires that several things be known or determined: first, the Hugoniot of the attenuator and the acceptor; second, the shock velocity (or pressure) attenuation as a function both of the initial velocity (or pressure) and the distance traveled in the attenuator; and third, the card-gap test results. These several areas are discussed in the following sections.

### 3.2.3.1 Plexiglas Hugoniot

The Hugoniot equation of state for Plexiglas that is used in the reduction of all sensitivity data under the SOPHY programs was determined at Aerojet (Reference 6). This equation is

$$U = 2.546 + 2.153\mu \quad (4)$$

where  $U$  is the shock velocity (mm/ $\mu$ sec) and  $\mu$  is the particle velocity (mm/ $\mu$ sec). With Plexiglas having a density ( $\rho_0$ ) of 1.186 gm/cm<sup>3</sup>, Equation 4 may be combined with  $P = 10\rho_0 U\mu$  to give these two equations:

$$P = 5.51 U^2 - 14.03U \quad (5)$$

and

$$P = 30.25\mu + 25.58\mu^2 \quad (6)$$

### 3.2.3.2 Propellant Hugoniot

The Hugoniot equations of state for AAB-3189 and -3225 were reported earlier (Reference 3). A small error in the computer program has since been discovered, and the following are the corrected Hugoniot of these formulations:

For AAB-3189 ( $\rho_0 = 1.725$  gm/cm<sup>3</sup>),

$$U = 1.89 + 2.63\mu \quad (7a)$$

$$P = 6.56 U^2 - 12.42 U \quad (7b)$$

$$P = 32.7\mu + 45.4\mu^2 \quad (7c)$$



For AAB-3225 ( $\rho_0 = 1.735 \text{ gm/cm}^3$ ),

$$U = 1.60 + 3.45\mu \quad (8a)$$

$$P = 5.03 U^2 - 8.07 U \quad (8b)$$

$$P = 27.8\mu + 59.8\mu^2 \quad (8c)$$

The Hugoniot equation for AAB-3267 adulterated propellant was determined by analyzing streak camera records of a shock wave passing through successive Plexiglas-propellant interfaces, as described in Reference 3. The resultant Hugoniot, obtained by the Hugoniot reflection method, is

$$P = 36.97\mu + 36.96\mu^2 \quad (9a)$$

from which the other equations can be derived, to give

$$U = 2.13 + 2.13\mu \quad (9b)$$

and

$$P = 8.15 U^2 - 17.4 U \quad (9c)$$

### 3.2.3.3 Shock-Pressure Attenuation in Plexiglas

In SOPHY I, the boosters were cast Composition B, and the acceptors were solid circular rods of Plexiglas, varying from 3-in. diameter to 6-in. diameter (Reference 2). In the present effort, the booster explosive is TNT because the card-gap tests include several large diameter samples, requiring large quantities of explosive, and TNT is the more suitable explosive for large boosters. The Plexiglas attenuator is composed of stacked square plates of Plexiglas. To achieve certain savings in test costs, the square shape was selected over the round. With sample diameter ranging from 6 to 42 in., it would be prohibitively expensive to conduct the tests with integral columns of Plexiglas; hence, the stacked-plate design.

Originally, the shock attenuation in the square-plate columns was to be determined optically with the standard test setup, including argon-bomb backlighting and the Beckman and Whitley streak camera. After performing several tests with streak-camera instrumentation, each of which

produced generally poor records, it was apparent that another method was required to obtain distance-time data. The adopted method used sets of two parallel enamelled-copper wires, at various interfaces in the Plexiglas column and at the Plexiglas-propellant interface, to obtain time-of-arrival data. This information was recorded on a rasteroscilloscope. The success of this method is demonstrated by excellent reproducibility and indicated by the smooth behavior of the distance-time data. The system appears to be limited, however, to sizes below 20 in., because the quality of the results deteriorated beyond that point. At the larger sizes, it was found that mechanical target probes inserted in spaced plates gave excellent time-of-arrival information.

The determination of shock attenuation in columns of Plexiglas 8-, 10-, 12-, 20-, 24-, and 42-in. square, by means of probes, is a significant advance in technology. The distance-time data are shown in Table 3. In Figures 14 through 19, the data are plotted along with the least-squares best-fit quadratic curve for each size Plexiglas column. The quadratic equations were differentiated to determine the velocity-distance data, which were transformed to pressure-distance by the Plexiglas Hugoniot equation.

This method was employed to reduce the data instead of the numerical differentiation method because the data were acquired at unequal increments in both variables. Numerical differentiation of such data is normally accomplished by differentiating the Lagrange or Hermite interpolation formulas, but no estimate of the error is possible when these formulas are applied, so the method is not particularly attractive. Also, these two methods do not function well when there is a large relative difference between successive intervals. Since the quadratic fits to the distance-time data do approximate the data closely, this method has been adopted.

The computed initial shock pressure  $P_0$  in Plexiglas from a TNT booster is estimated, from the differentiated fits to the square-column data, to be 118 kbar.

A comparison of the  $P/P_0$  versus  $x/d$  data obtained from these fits with the corresponding curve derived from the SOPHY I study (Reference 2) is shown in Figure 20. Here,  $P$  is the shock pressure,  $x$  is the distance traveled in Plexiglas, and  $d$  is the diameter of the circular column or the length of a side of the square plate. The excellent graphical correlation shows that the attenuation process is essentially determined by the initial

Table 3. Attenuation of Shock from TNT Booster by  
Stacked Squares of Plexiglas.

Plexiglas Column Cross-Section (in.)	Distance Traveled in Plexiglas (in.)	Time of Arrival ( $\mu$ sec)
8 x 8	1.00	4.37
	1.31	6.25
	2.00	9.44
	2.81	14.05
	3.00	14.63
	3.53	17.5
	4.00	20.1
	4.28	22.2
	5.00	25.6
	6.47	34.85
10 x 10	6.70	37.5
	7.25	40.9
	3.00	14.4
	4.00	19.5
	5.00	25.0
	7.00	37.0
	7.57	41.1
	8.52	47.5
12 x 12	9.50	55.5
	10.00	59.5
	2.00	9.0
	5.00	25.0
	9.75	54.3
	10.80	61.1
20 x 20	11.00	63.0
	11.80	70.7
	7.00	35.0
	9.50	52.5
	13.50	70.0
24 x 24	16.50	92.1
	18.50	107.0
	20.65	137.5
42 x 42	11.75	60.0
	23.50	136.0
	25.00	125.6
	27.10	142.0
	31.00	166.8
	32.70	177.0
	34.75	191.5
	38.70	220.0
	40.50	235.5
	42.00	248.0

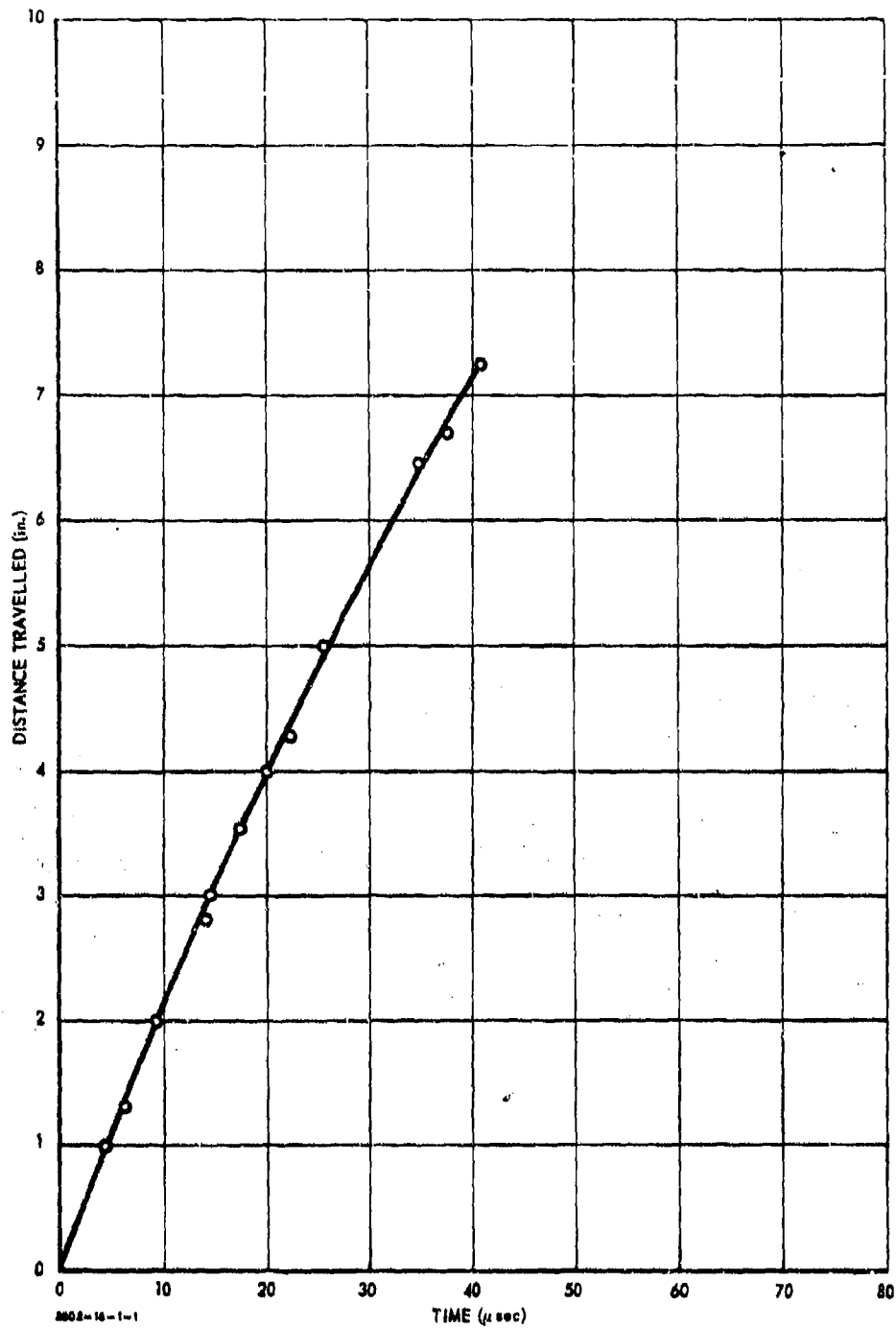


Figure 14. Attenuation in 8-in. Squares of Stacked Plexiglas Plates.

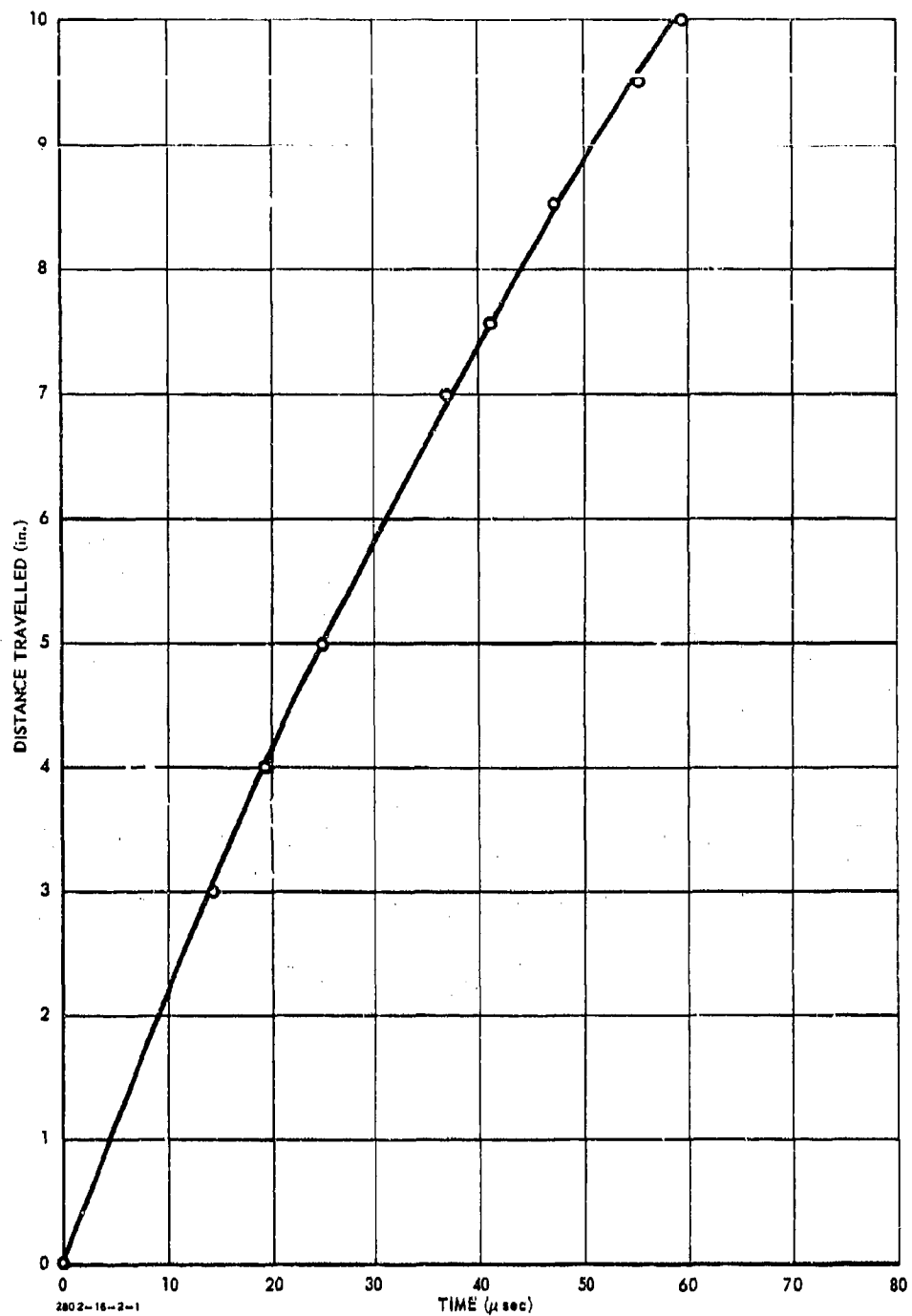


Figure 15. Attenuation in 10-in. Squares of Stacked Plexiglas Plates.

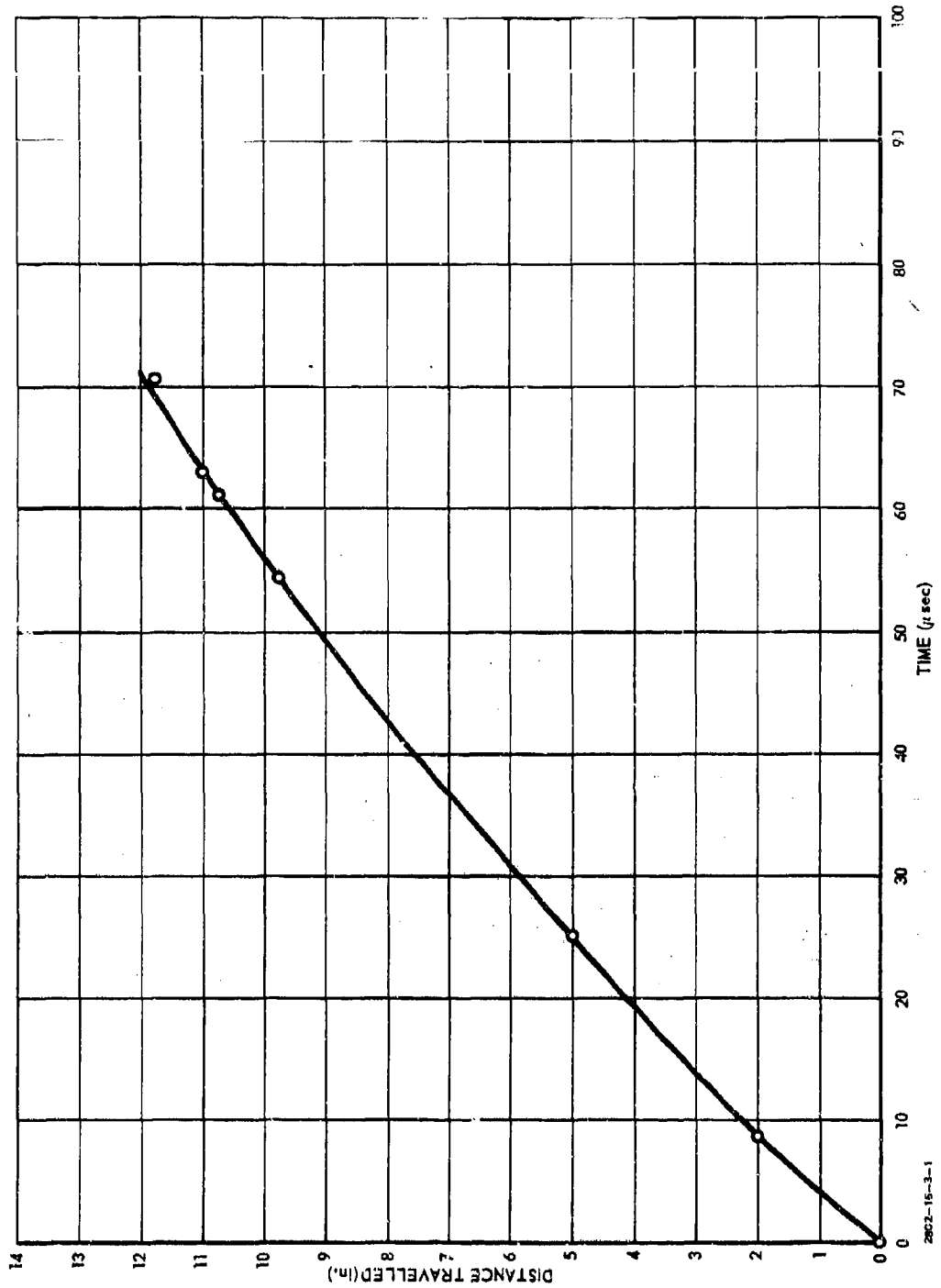
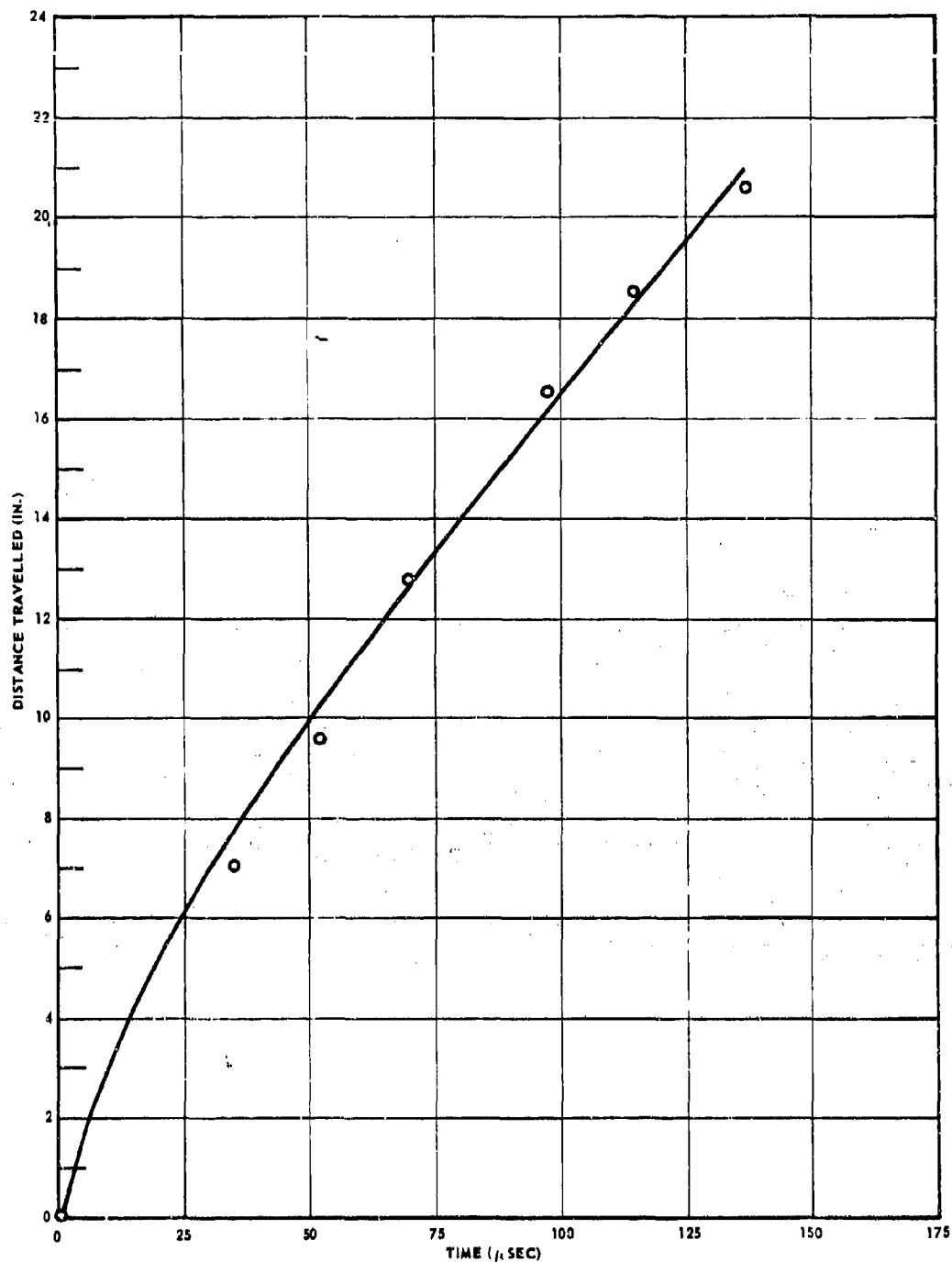
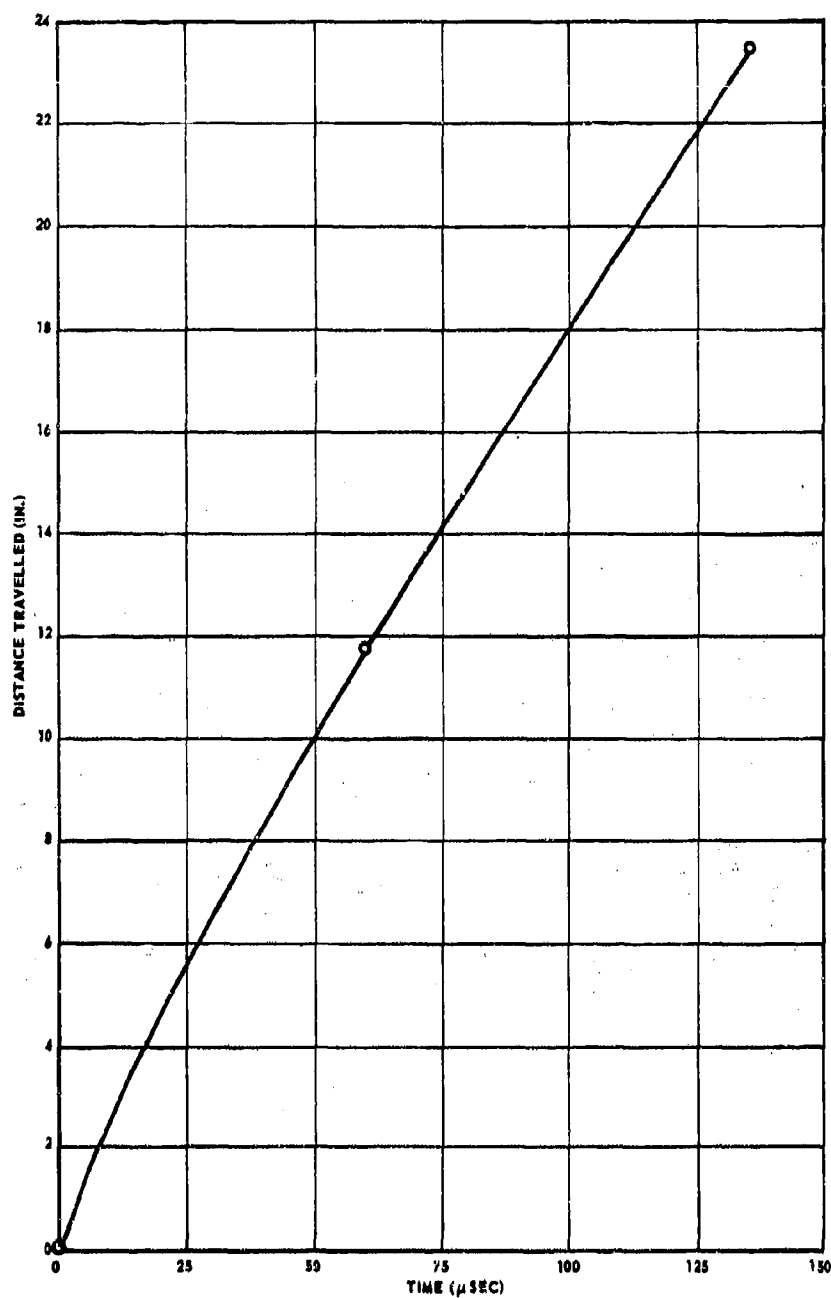


Figure 16. Attenuation in 12-in. Squares of Stacked Plexiglas Plates.



28 42-6-17-1  
Figure 17. Attenuation in 20-in. Squares of Stacked Plexiglas Plates.



2042-S-10-1

Figure 18. Attenuation in 24-in. Squares of Stacked Plexiglas Plates.



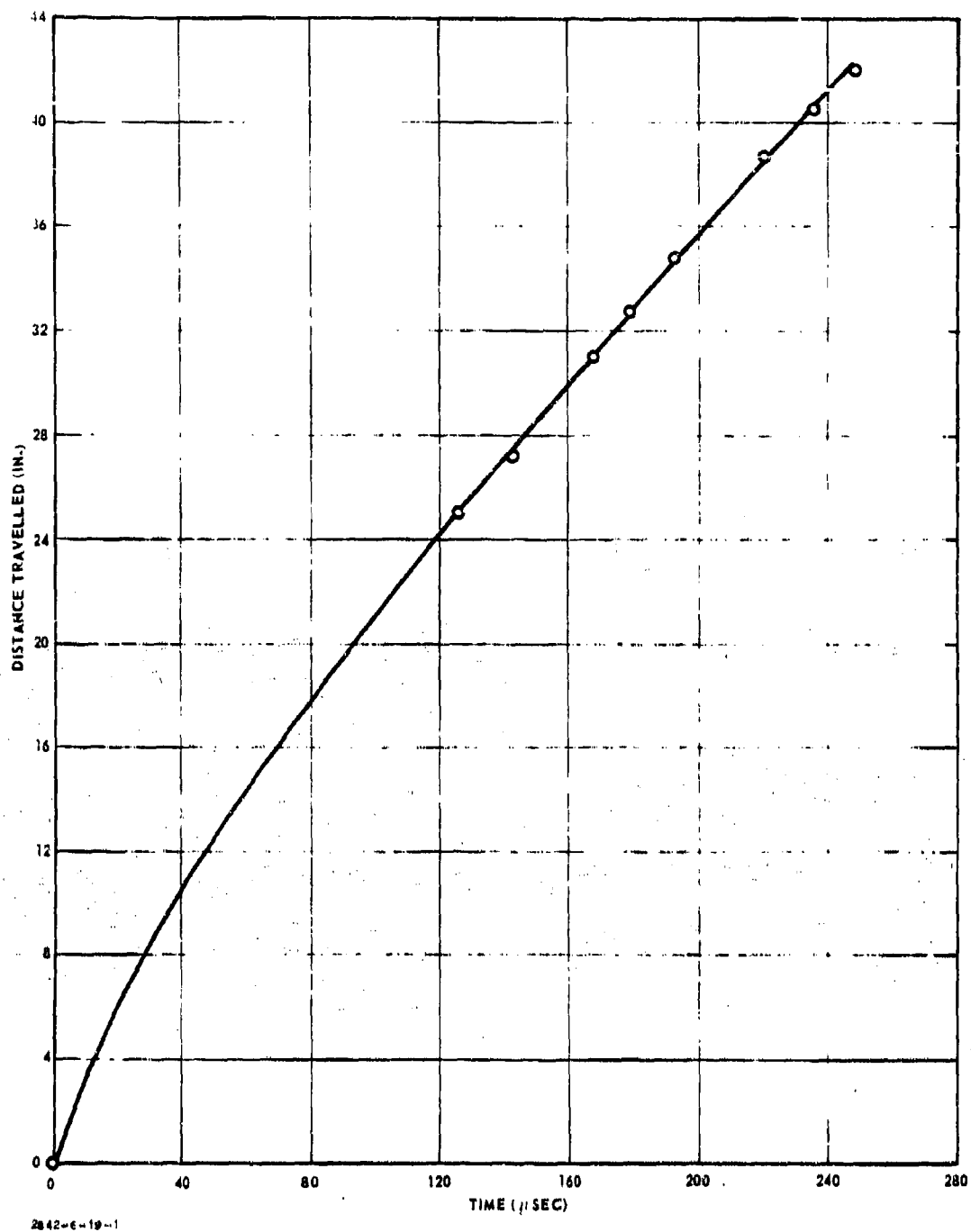


Figure 19. Attenuation in 42-in. Squares of Stacked Plexiglas Plates.

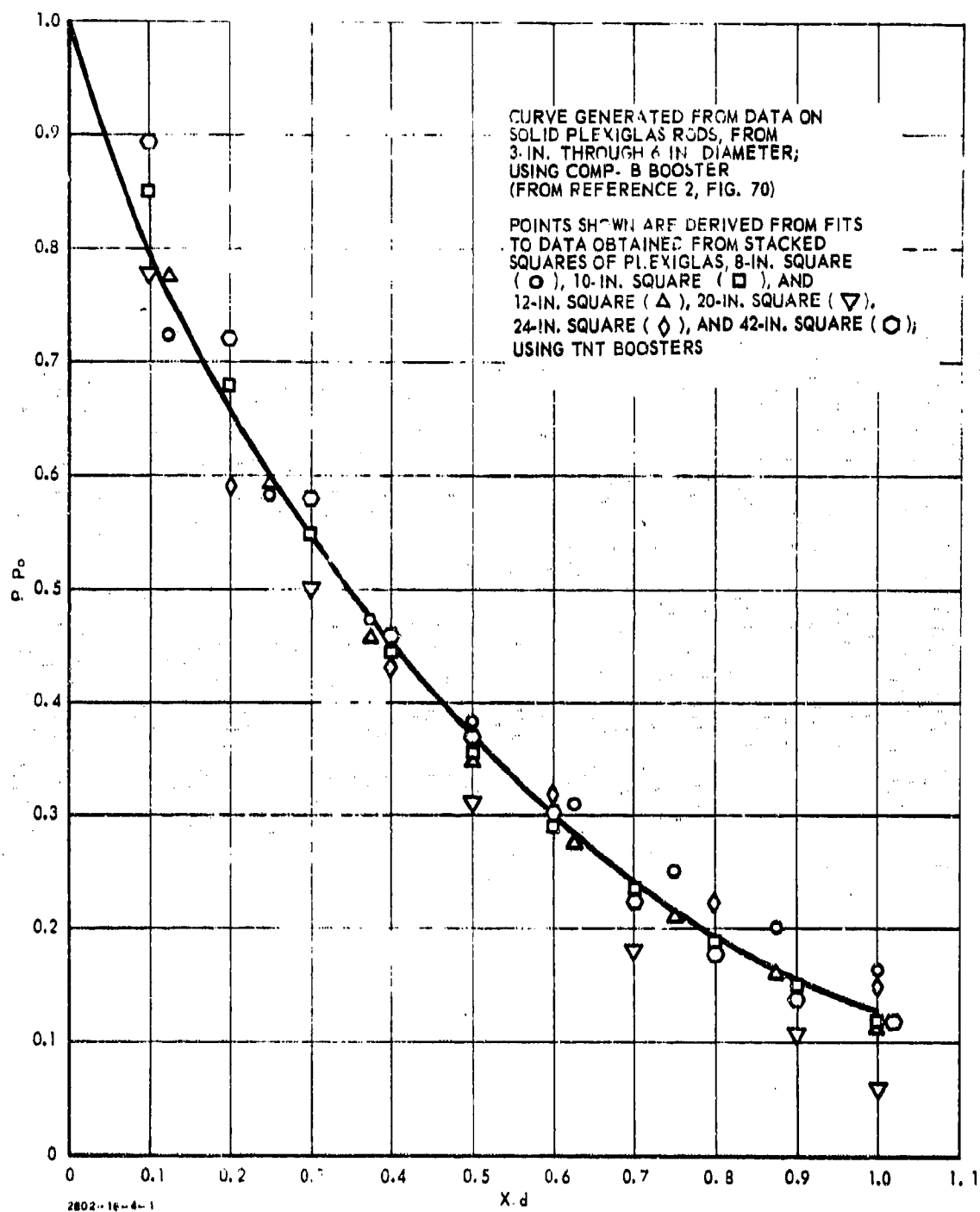


Figure 20. Correlation of Shock Pressure Attenuation Data.

shock pressure and two geometrical parameters; i. e., the distance traveled and the cross-sectional dimension of the attenuator column. Since the SOPHY I attenuation curve also is fit by previously obtained data from Plexiglas columns as small as 1/2-in. diameter, it holds over an 84-fold range.

#### 3.2.3.4 Card-Gap Tests

Plexiglas card-gap tests are conducted in the standard manner by testing whether a certain thickness of Plexiglas attenuates the shock wave delivered by a high-explosive booster to a level insufficient to initiate a supercritical cylindrical acceptor charge. If detonation is not achieved, less Plexiglas is used in the next test. This sequence continues until a thickness is found that allows detonation to be initiated. At this point the sequence reverses, using smaller incremental changes in the Plexiglas thickness, until no detonation occurs. The process again is reversed. The testing continues in this fashion, decreasing the increments after each reversal, until the go-no-go range has been reduced to the desired limit.

The results of the card-gap tests, performed in this subtask at certain diameters, bracket  $P^+$  within a 5 to 6 kbar range, which is the largest range in all the data. In general, at the other diameters,  $P^+$  has been bracketed within 1 to 2 kbars. The results of the card-gap tests define the initiation criteria of these propellants quite adequately.

These results are given in Tables 4 through 6. The initiation criteria for the three propellants are shown individually in Figures 21 through 23, and are combined (using a reduced-diameter abscissa,  $d/d_c$ ) in Figure 24.

#### 3.2.3.5 Extrapolation to Unadulterated Propellant

From Figure 24, it is clear that  $P^+$  at the critical diameter decreases as the critical diameter is increased. The estimates of  $P^+$  are, in order of increasing critical diameters, 62, 37, and 34 kbar. The last value is extremely tentative because of the lack of sufficient data with the AAB-3267 material. Nevertheless, it is clear that the rate at which  $P^+$  at the critical diameter is decreasing, with respect to the weight fraction RDX, is diminishing rapidly. Assuming a monotonic behavior, the  $P^+$  for unadulterated propellant could be 20 to 25 kbar, at the critical diameter.

Table 4. Card-Gap Test Results, AAB-3189 Propellant.

Propellant Diameter (in.)	Plexiglas Thickness (dia)	Incident Pressure in Plexiglas* (kbar)	Transmitted Pressure in Propellant* (kbar)	Test Result	Test Number
10	0.762	25	28	Go	3.3.5.21
	0.856	20	22	Go	3.3.5.22
	0.856	20	22	Go	3.3.5.24
	0.950	17	19	No go	3.3.5.20
	0.950	17	19	No go	3.3.4.23
12	0.823	22	25	Go	3.3.5.26
	0.907	20	22	Go	3.3.5.27
	0.907	20	22	Go	3.3.5.29
	0.979	16	18	No go	3.3.5.25
	0.979	16	18	No go	3.3.5.28
*At Plexiglas-propellant interface.					

Table 5. Card-Gap Test Results,  
AAB-3225 Propellant.

Propellant Diameter (in.)	Plexiglas Thickness (dia)	Incident Pressure in Plexiglas* (kbar)	Transmitted Pressure in Propellant* (kbar)	Test Result	Test Number
6	0.618	34	41	Go	3.3.5.1
	0.742	26	31	Go	3.3.5.3
	0.809	23	27	Go	3.3.5.11
	0.816	22	26	No go	3.3.5.7
	0.840	21	24	No go	3.3.5.9
	0.860	20	23	No go	3.3.5.2
7	0.778	24	28	Go	3.3.5.14
	0.833	21	24	Go	3.3.5.15
	0.858	20	23	Go	3.3.5.18
	0.889	19	22	No go	3.3.5.13
8	0.881	19	22	Go	3.3.5.4
	0.925	18	21	Go	3.3.5.10
	0.956	17	20	No go	3.3.5.8
	1.000	15	17	No go	3.3.5.6
	1.112	13	15	No go	3.3.5.5
12	0.823	22	26	Go	3.3.5.31
	0.901	18	21	Go	3.3.5.52
	0.912	18	21	Go	3.3.5.32
	0.995	15	17	No go	3.3.5.51
	1.073	11	16	No go	3.3.5.30
20	0.828	22	26	Go	3.3.5.33
	0.922	18	21	Go	3.3.5.35
	0.956	17	20	Go	3.3.5.39
	0.969	16	19	Go	3.3.5.53
	1.017	15	17	No go	3.3.5.34
24	0.896	19	22	Go	3.3.5.37
	0.938	17	20	Go	3.3.5.38
	0.938	17	20	Go	3.3.5.54
	0.977	16	18	No go	3.3.5.36
	0.977	16	18	No go	3.3.5.50
*At Plexiglas-propellant interface.					

Table 6. Card-Gap Test Results, AAB-3267 Propellant.

Propellant Diameter (in.)	Plexiglas Thickness (dia)	Incident Pressure in Plexiglas* (kbar)	Transmitted Pressure in Propellant* (kbar)	Test Result	Test Number
12	0.646	32	38	Go	3.3.5.57
	0.732	27	32	No go	3.3.5.58
	0.818	22	26	No go	3.3.5.56
42	0.914	16	18	Go	3.3.5.59
	0.966	14	16	Go	3.3.5.60
	1.006	12	14	No go	3.3.5.55
*At Plexiglas-propellant interface.					

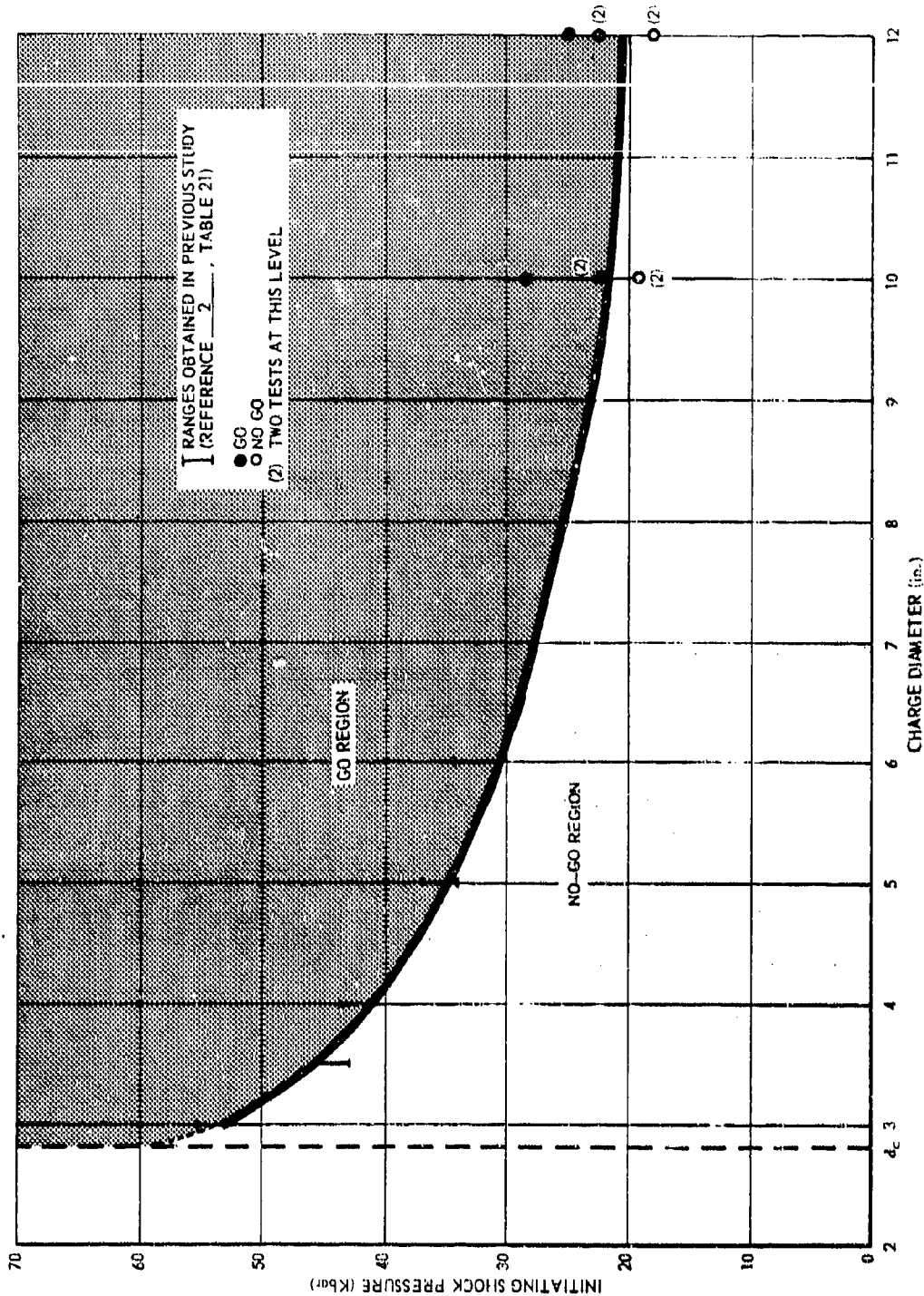


Figure 21. Initiation Criterion for AAB-3189.

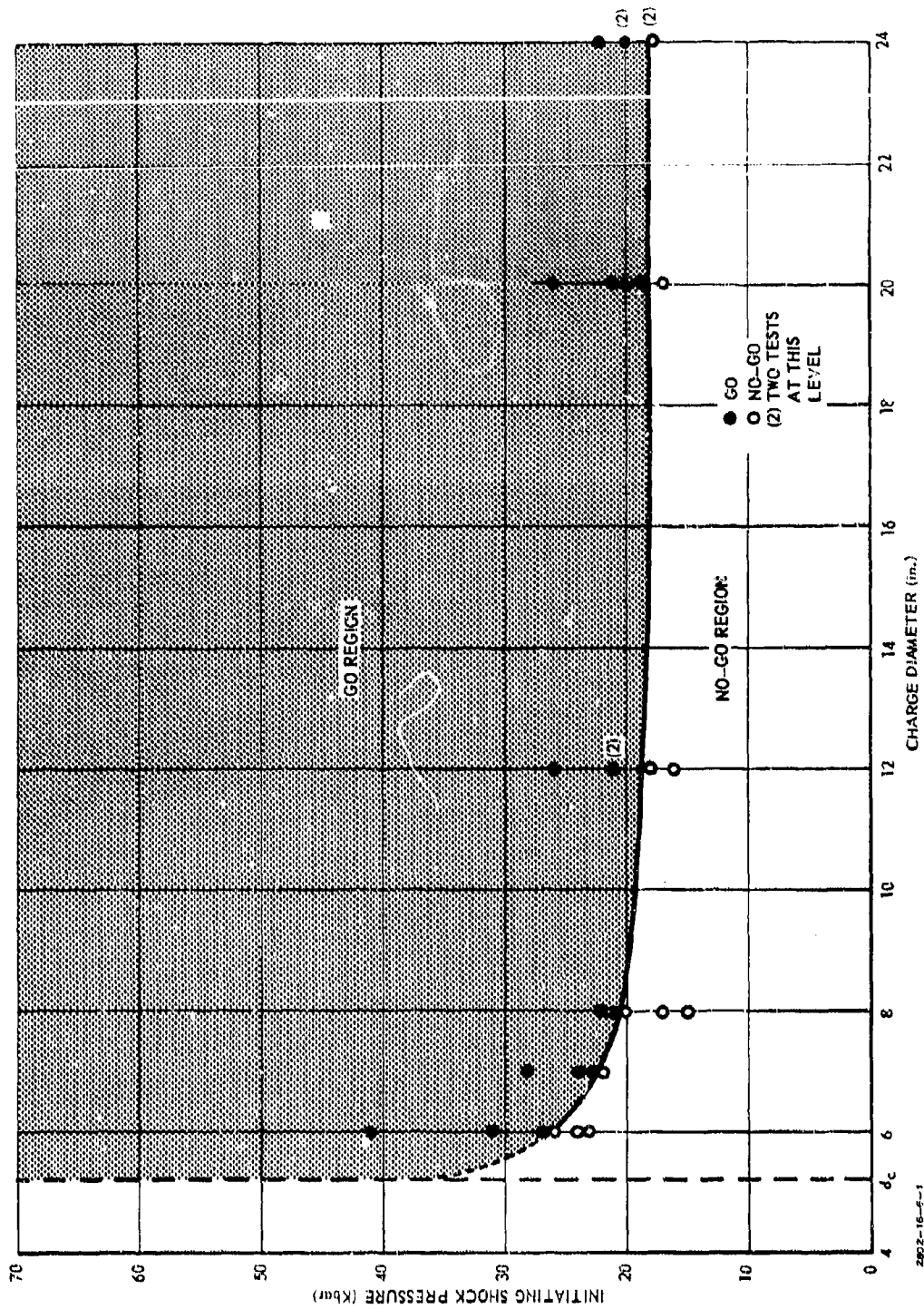


Figure 22. Initiation Criterion for AAB-3225.



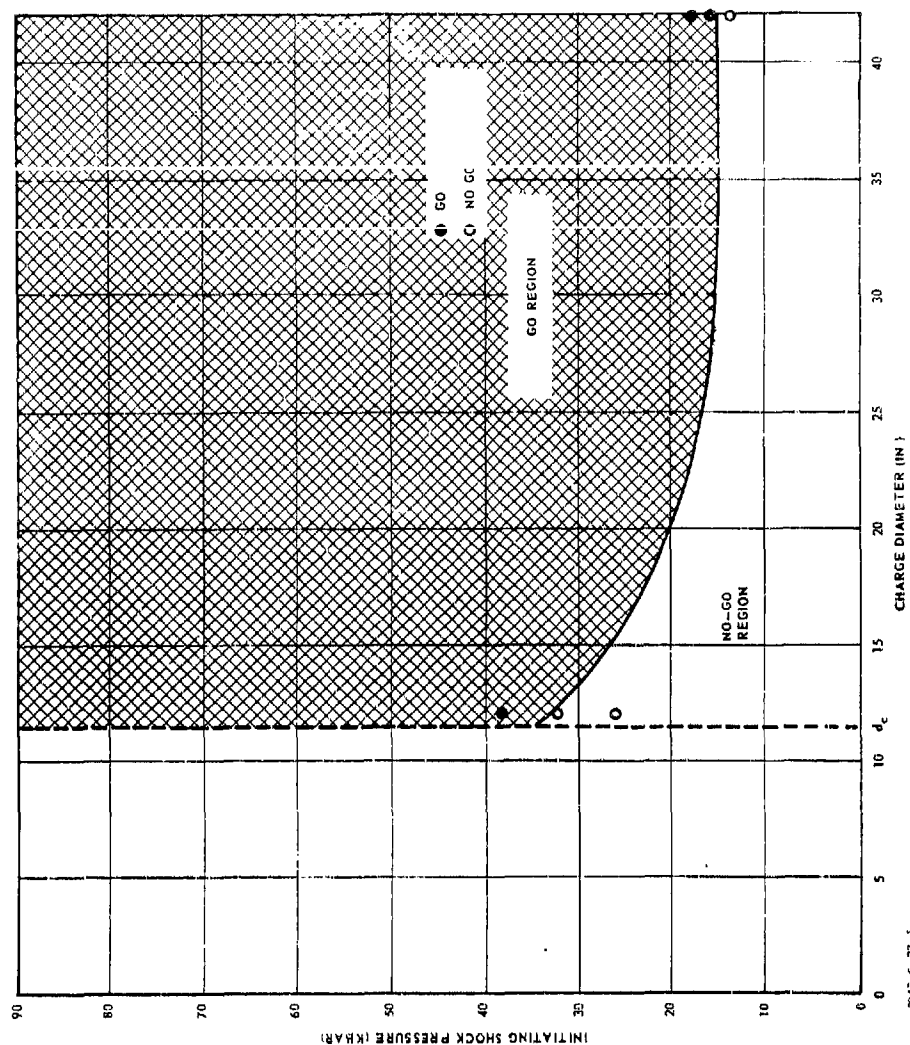


Figure 23. Initiation Criterion for AAB-2267.

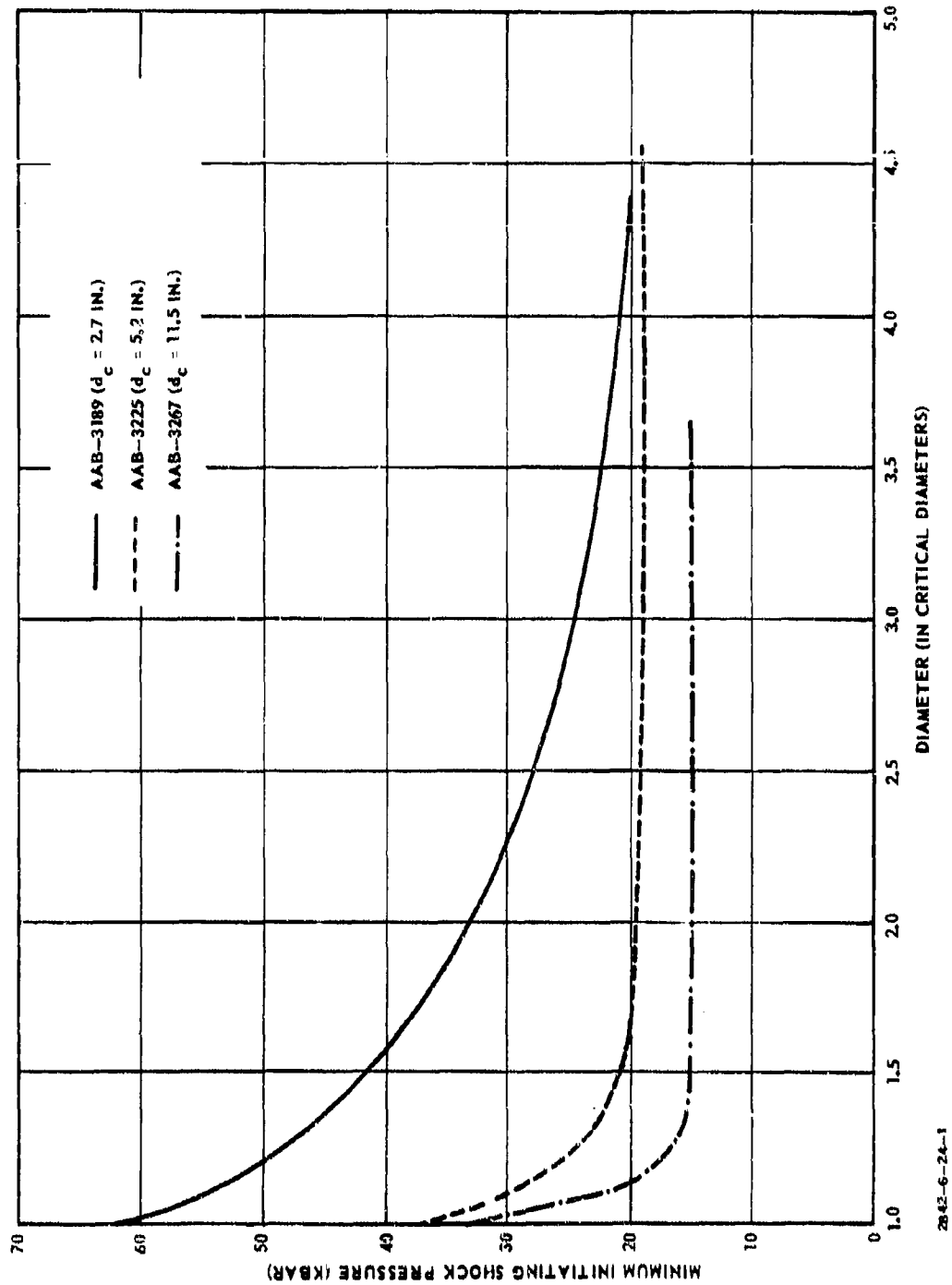


Figure 24. Normalized Initiation Criterion.

$P^*$  is the minimum  $P^+$ , approached as  $d$  increases to the ideal diameter. From Figure 24, the various estimates of  $P^*$  -- 20 kbar for AAB-3189, 19 kbar for AAB-3225, and 15 kbar for AAB-3267 -- are quite close to each other. By extrapolating the gradual decrease in  $P^*$  with decreasing RDX, the  $P^*$  for unadulterated propellant may be 8 to 10 kbar.

These estimates of two points on the initiation criterion for unadulterated propellant receive some support regarding their general magnitude from another analysis. It is observed that, at the critical diameter,  $P^+$  is very close to the spike detonation pressure calculated from the  $P(U)$  Hugoniot equation at  $U = U_c$ , the detonation velocity of a sample at critical diameter. For AAB-3189,  $P^+$  is 62 kbar, and the computed spike detonation pressure is 65 kbar. For AAB-3225,  $P^+$  is estimated to be 37 kbar, and the computed spike detonation pressure is 50 kbar. For AAB-3267,  $P^+$  is estimated to be 34 kbar, and the computed spike detonation pressure is 48 kbar. From the results of the 72-in. critical-diameter test of ANB-3226 (unadulterated propellant), the detonation velocity was 3.2 mm per  $\mu$ sec (Reference 7). Assuming that the  $P(U)$  Hugoniots for AAB-3267 and ANB-3226 are the same for  $P < 25$  kbar, which has been the case for the three adulterated formulations, the spike detonation pressure of ANB-3226 can be estimated. For the 72-in. diameter sample, this estimate is 29 kbar. Since the 72-in. diameter is greater than or equal to the critical diameter, 29 kbar is greater than or equal to the spike detonation pressure at the critical diameter and is therefore an upper bound on the estimated value of  $P^+$  at critical diameter.

#### 3.2.4 Sensitivity of Unadulterated Propellant (Subtask 3.3.6)

This subtask investigates the use of an axial resistance-type probe in subcritical samples to determine  $P^*$ . In SOPHY I, a series of tests was performed to evaluate the initiation criterion (Reference 2). By using small diameter boosters on supercritical samples, the initial size of the shock wave was varied to find the smallest diameter booster that would initiate the propellant. In cases where the shock wave was too small to initiate detonation, it was observed that, for the first diameter along the acceptor axis, the velocity of the shock wave was essentially equal to the detonation velocity. The wave attenuates more rapidly at farther distances from the axis.

This phenomenon suggested that a subcritical sample, explosively shocked, may appear to sustain detonation momentarily along its axis before the rarefaction losses abort the reaction. The material at the charge axis would react to a given pressure stimulus in a manner that would be independent of the size of the sample, for a very short time.

The problem is to monitor the velocity at the charge axis continuously, and by varying the input shock pressure, to determine the minimum pressure that causes a temporary sustainment in velocity. To monitor the axial velocity, resistance probes were cast at the axis of 2-in. diameter samples of AAB-3189 propellant and similarly in ANB-3226 samples of 6-, 12-, and 24-in. diameter.

The probe is electronically in series with a fixed resistor in a constant-voltage dc circuit, and the voltage across the fixed resistor is fed to an oscilloscope. The changing effective length of the axis resistor, as the ionized shock front moves down the charge, reduces the resistance of the probe and causes an increase in the voltage across the fixed resistor. Thus, the output trace can be easily related to the distance-time behavior of the shock wave.

The first phase consisted of testing the AAB-3189 samples to determine the validity of the assumptions that had been made. Card-gap techniques were applied to vary the shock pressure, in the region from less than 20 to more than 100 kbar. The results were not those that had been expected. The shape of the pulse, even when no attenuation was used in the test, indicates that there were several uncontrolled factors involved, because a literal reduction of the data leads to highly unrealistic shock velocities. Furthermore, there was no evidence found that could identify a pressure level below which the propellant behaved differently. Thus, it was impossible to determine a pressure to be compared to  $P^*$  as determined from supercritical card-gap tests.

The probe system was checked with a detonating material, Composition B, and a linear trace was generated. While the system operates well where there is sustained detonation at high velocity, it does not function acceptably in the transient, subcritical region. It must be concluded that the method proposed to determine  $P^*$  from subcritical samples will not work. On this basis, the tests with ANB-3226 have been canceled.

Since the difficulty may have been due to limitations in the ability of this probe design to function properly, it is possible that another method could be developed that would use subcritical samples to determine  $P^*$ . The high interest in knowing  $P^*$  for unadulterated propellant justifies further research effort in exploring the subcritical samples as a source of this information. Many small-scale tests can be performed to evaluate various approaches at less cost than would be incurred by a series of supercritical card-gap tests to bracket  $P^+$  at a specific diameter.

#### 4. PROPELLANT DEFECTS STUDY

A summary report on the progress achieved in developing methods to synthesize and characterize porous and cracked propellant has been prepared by project personnel in the Propellant Development Department, Research and Technology Operations, at Aerojet's Sacramento Plant. This report will be included in the final report under this contract.

#### 5. FUTURE WORK

A 2-1/2-month extension of the contract at no additional cost has been proposed, which will include investigation of three additional areas: (1) the effect of other published Hugoniot for Plexiglas on the derived initiation criteria for adulterated propellants, (2) evaluation of the initiation criterion for AAB-3189 by testing 6-in. cylindrical samples, and (3) evaluation of the initiation criterion for AAB-3189 applied to rectangular cross-section shapes.

##### 5.1 PLEXIGLAS HUGONIOT

There are several published Hugoniot equations of state for Plexiglas, Lucite, or Perspex, which are trade names for polymethylmethacrylate. These Hugoniot differ from one another, and there is no completely objective basis for determining the one that is most accurate. The Plexiglas Hugoniot is required to determine the propellant Hugoniot and the shock pressure attenuation in Plexiglas, and it is also required to calculate the shock pressure transmitted in propellant from knowledge of the shock pressure in Plexiglas incident to the Plexiglas-propellant interface.

Each of the published Hugoniot will be used with the data obtained in this program to calculate the effect on the initiation criterion values. If the final results agree sufficiently well with values obtained using the Aerojet Hugoniot equation, there will be no reason to analyze the situation further. However, if significant differences are found, it will be necessary to determine the relative merits of the various Hugoniots, particularly with respect to the range over which they were determined and the method to obtain the Hugoniots. If the investigation so indicates, the initiation criteria will be reported in several forms, as reduced from the respective Plexiglas Hugoniot equations. The criteria then will be subject to further definition of the Hugoniot equation for Plexiglas.

## 5.2 EVALUATION OF INITIATION CRITERION

### 5.2.1 Cylinders

The initiation criterion of AAB-3189 will be evaluated using cylindrical samples. High-explosive boosters of various diameters will be used to apply input shock waves of different initial areas and pressures into 6-in. diameter acceptors. The acceptors will be instrumented to provide data from which the shape of the wave and the pressure profile can be calculated at any time in the history of the wave. The data then will be plotted as average pressure  $\bar{P}$  vs  $A$ , against the corresponding initiation criterion, to determine whether the hypothesis of the initiation criterion is honored.

### 5.2.2 Rectangles

The initiation criterion is postulated to be a property of the material and not dependent on the shape of the test sample. The initiation criterion is therefore defined as that portion of the go region in which  $A > A_c$ , the cross-sectional area of the critical size of any particular shape. This hypothesis will be studied in two ways: First, a series of tests will be conducted to evaluate the initiation criterion as described in Section 5.2.1. Second, highly instrumented card-gap tests will be performed on rectangles of width equal to two thicknesses. The  $P^+$  near critical should be less than 50 kbar since the critical cross-sectional area is 8 in.<sup>2</sup> (see Figure 85, Reference 2). The shock wave will not be a plane wave, so its area will exceed 8 in.<sup>2</sup>, and  $P^+$  should then be less than 50 kbar. If the hypothesis is wrong, that is, if  $P^+$  should be found to be greater than 50 kbar, the initiation criterion will have to be redefined for the rectangular shape.

#### REFERENCES

1. Program Plan, Project SOPHY, Solid Propellant Hazards Program. Aerojet-General Corporation Report 0977-01(01)ER, 14 December 1965.
2. Large Solid-Propellant Boosters Explosive Hazards Study Program (Project SOPHY). Technical Documentary Report AFRPL-TR-65-211, Aerojet-General Corporation Report 0866-01(01)FP, 24 November 1965.
3. Project SOPHY, Solid Propellant Hazards Program. Technical Documentary Report AFRPL-TR-66-276, Aerojet-General Corporation Report 0977-01(05)QP, 31 December 1966.
4. Project SOPHY, Solid Propellant Hazards Program. Technical Documentary Report AFRPL-TR-66-26, Aerojet-General Corporation Report 0977-01(04)QP, 29 September 1966.
5. Salzman, P. K. "Determination of the Maximum Transmitted Shock at the Interface Between Two Condensed Media," AIAA Journal, Vol. 2, No. 2, pp 359-360 (1964).
6. Analysis of Shock Attenuation for 0.5- and 2.0-Inch Diameter Card-Gap Sensitivity Tests. Aerojet-General Corporation Special Report, IWA 3646-10-458, October 1961.
7. Project SOPHY, Solid Propellant Hazards Program. Technical Documentary Report AFRPL-TR-66-25, Aerojet-General Corporation Report 0977-01(03)QP, 28 June 1966.

UNCLASSIFIED

DOCUMENT CONTROL DATA - R&D		
<i>(Security classification of title, body of abstract and indexing annotation must be entered when the overall report is classified)</i>		
1. ORIGINATING ACTIVITY (Corporate author)		2a. REPORT SECURITY CLASSIFICATION
Aerojet-General Corporation Downey, California 90241		Unclassified
		2b. GROUP
		N/A
3. REPORT TITLE		
Project SOPHY - Solid Propellant Hazards Program		
4. DESCRIPTIVE NOTES (Type of report and inclusive dates)		
Progress Report 1 December 1966 - 28 February 1967		
5. AUTHOR(S) (Last name, first name, initial)		
Elwell, R. B. Salzman, P. K. Weatherill, W. T.		
6. REPORT DATE	7a. TOTAL NO. OF PAGES	7b. NO. OF PAGES
March 1967	61	7
8a. CONTRACT OR GRANT NO.	8b. ORIGINATOR'S REPORT NUMBER(S)	
AF04(611)10919	0977-01(1) DP	
9. PROJECT NO.	9c. OTHER REPORT NO(S) (Any other numbers that may be assigned this report)	
63A00201	AFRPL-TR-67-67	
10. AVAILABILITY/LIMITATION NOTICES		
Qualified requestors may obtain copies of this report from DDC.		
11. SUPPLEMENTARY NOTES		12. SPONSORING MILITARY ACTIVITY
		AFRPL, Hazards Analysis Branch, AF Systems Command, Edwards AFB Edwards, California 93523
13. ABSTRACT		
<p>Verification that the sustainment theory of critical geometry can be applied to an adulterated propellant different from that by which the theory was originally developed has been obtained from tests of square column and hollow-core cylindrical shapes. The effect of pulse width on the minimum shock pressure required to initiate detonation has been determined experimentally by flyer-plate tests. The initiation criteria for three different RDX-adulterated PBAN-type propellants have been determined. From these, the minimum shock pressure required to initiate detonation of unadulterated propellant is predicted to be approximately 20 kbar at critical diameter and 10 kbar at ideal diameter.</p>		

DD FORM 1473

UNCLASSIFIED



14. KEY WORDS	LINK A		LINK B		LINK C	
	ROLE	WT	ROLE	WT	ROLE	WT
Sensitivity Primers Kinetic energy Temperature						

INSTRUCTIONS

1. ORIGINATING ACTIVITY: Enter the name and address of the contractor, subcontractor, grantee, Department of Defense activity or other organization (*corporate author*) issuing the report.

2a. REPORT SECURITY CLASSIFICATION: Enter the overall security classification of the report. Indicate whether "Restricted Data" is included. Marking is to be in accordance with appropriate security regulations.

2b. GROUP: Automatic downgrading is specified in DoD Directive 5200.10 and Armed Forces Industrial Manual. Enter the group number. Also, when applicable, show that optional markings have been used for Group 3 and Group 4 as authorized.

3. REPORT TITLE: Enter the complete report title in all capital letters. Titles in all cases should be unclassified. If a meaningful title cannot be selected without classification, show title classification in all capitals in parenthesis immediately following the title.

4. DESCRIPTIVE NOTES: If appropriate, enter the type of report, e.g., interim, progress, summary, annual, or final. Give the inclusive dates when a specific reporting period is covered.

5. AUTHOR(S): Enter the name(s) of author(s) as shown on or in the report. Enter last name, first name, middle initial. If military, show rank and branch of service. The name of the principal author is an absolute minimum requirement.

6. REPORT DATE: Enter the date of the report as day, month, year, or month, year. If more than one date appears on the report, use date of publication.

7a. TOTAL NUMBER OF PAGES: The total page count should follow normal pagination procedures, i.e., enter the number of pages containing information.

7b. NUMBER OF REFERENCES: Enter the total number of references cited in the report.

8a. CONTRACT OR GRANT NUMBER: If appropriate, enter the applicable number of the contract or grant under which the report was written.

8b, 8c, & 8d. PROJECT NUMBER: Enter the appropriate military department identification, such as project number, subproject number, system numbers, task number, etc.

9a. ORIGINATOR'S REPORT NUMBER(S): Enter the official report number by which the document will be identified and controlled by the originating activity. This number must be unique to this report.

9b. OTHER REPORT NUMBER(S): If the report has been assigned any other report numbers (*either by the originator or by the sponsor*), also enter this number(s).

10. AVAILABILITY/LIMITATION NOTICES: Enter any limitations on further dissemination of the report, other than those imposed by security classification, using standard statements such as:

(1) "Qualified requesters may obtain copies of this report from DDC."

(2) "Foreign announcement and dissemination of this report by DDC is not authorized."

(3) "U. S. Government agencies may obtain copies of this report directly from DDC. Other qualified DDC users shall request through \_\_\_\_\_."

(4) "U. S. military agencies may obtain copies of this report directly from DDC. Other qualified users shall request through \_\_\_\_\_."

(5) "All distribution of this report is controlled. Qualified DDC users shall request through \_\_\_\_\_."

If the report has been furnished to the Office of Technical Services, Department of Commerce, for sale to the public, indicate this fact and enter the price, if known.

11. SUPPLEMENTARY NOTES: Use for additional explanatory notes.

12. SPONSORING MILITARY ACTIVITY: Enter the name of the departmental project office or laboratory sponsoring (*paying for*) the research and development. Include address.

13. ABSTRACT: Enter an abstract giving a brief and factual summary of the document indicative of the report, even though it may also appear elsewhere in the body of the technical report. If additional space is required, a continuation sheet shall be attached.

It is highly desirable that the abstract of classified reports be unclassified. Each paragraph of the abstract shall end with an indication of the military security classification of the information in the paragraph, represented as (TS), (S), (C), or (U).

There is no limitation on the length of the abstract. However, the suggested length is from 150 to 225 words.

14. KEY WORDS: Key words are technically meaningful terms or short phrases that characterize a report and may be used as index entries for cataloging the report. Key words must be selected so that no security classification is required. Identifiers, such as equipment model designation, trade name, military project code name, geographic location, may be used as key words but will be followed by an indication of technical context. The assignment of links, rules, and weights is optional.